

THEORETICAL AND EXPERIMENTAL INVESTIGATION ON  
CHARACTERISTICS OF ADSORPTION COOLING SYSTEMS USING  
ADVANCED POROUS MATERIALS

A THESIS SUBMITTED TO  
THE GRADUATE SCHOOL OF NATURAL AND APPLIED SCIENCES  
OF  
MIDDLE EAST TECHNICAL UNIVERSITY

BY

NIMA BONYADI

IN PARTIAL FULFILLMENT OF THE REQUIREMENTS  
FOR  
THE DEGREE OF MASTER OF SCIENCE  
IN  
MECHANICAL ENGINEERING

SEPTEMBER 2014



Approval of the thesis:

**THEORETICAL AND EXPERIMENTAL INVESTIGATION ON  
CHARACTERISTICS OF ADSORPTION COOLING SYSTEMS USING  
ADVANCED POROUS MATERIALS**

submitted by **NIMA BONYADI** in partial fulfillment of the requirements for the degree of **Master of Science in Mechanical Engineering Department, Middle East Technical University** by,

Prof. Dr. Canan ÖZGEN  
Dean, Graduate School of **Natural and Applied Sciences**

\_\_\_\_\_

Prof. Dr. Tuna BALKAN  
Head of Department, **Mechanical Engineering**

\_\_\_\_\_

Assoc. Prof. Dr. Cemil YAMALI  
Supervisor, **Mechanical Engineering Department, METU**

\_\_\_\_\_

Assoc. Prof. Dr. Derek K. BAKER  
Co-supervisor, **Mechanical Engineering Department, METU**

\_\_\_\_\_

**Examining Committee Members:**

Prof. Dr. Kahraman ALBAYRAK  
Mechanical Engineering Department, METU

\_\_\_\_\_

Assoc. Prof. Dr. Cemil YAMALI  
Mechanical Engineering Department, METU

\_\_\_\_\_

Assoc. Prof. Dr. Derek K. BAKER  
Mechanical Engineering Department, METU

\_\_\_\_\_

Prof. Dr. Mecit SIVRIOĞLU  
Mechanical Engineering Department, Gazi University

\_\_\_\_\_

Dr. Tahsin ÇETİNKAYA  
Mechanical Engineering Department, METU

\_\_\_\_\_

**Date:**

\_\_\_\_\_

**I hereby declare that all information in this document has been obtained and presented in accordance with academic rules and ethical conduct. I also declare that, as required by these rules and conduct, I have fully cited and referenced all material and results that are not original to this work.**

Name, Last Name: NIMA BONYADI

Signature :

# ABSTRACT

## THEORETICAL AND EXPERIMENTAL INVESTIGATION ON CHARACTERISTICS OF ADSORPTION COOLING SYSTEMS USING ADVANCED POROUS MATERIALS

BONYADI, NIMA

M.S., Department of Mechanical Engineering

Supervisor : Assoc. Prof. Dr. Cemil YAMALI

Co-Supervisor : Assoc. Prof. Dr. Derek K. BAKER

September 2014, 75 pages

The solid sorption cooling systems are getting more popular around the globe due to their benign behavior and possibility to work with renewable energy. Despite many advantages, the overall efficiency of adsorption cooling systems is still low in comparison to vapor compression chillers. Researchers declare that heat and mass transfer and adsorption capacity inside the adsorbent bed have dominant role on the performance of the cooling unit. One way to increase both adsorption capacity and heat distribution inside the bed is by improving the characteristics of the adsorbents. Enhancing the adsorption characteristics of adsorbent materials can be achieved by developing new composites and mixtures. Using impregnation method and metal piece additives increase the adsorption capacity and thermal conductivity of the adsorbent.

This thesis is an integration of three related works. In the first place, the influence of thermal conductivity on adsorption and desorption processes were investigated numerically. Next, the silica gel adsorbent was modified using metal mixture and impregnation methods. In the last step, the thermo physical and adsorption properties of new materials like adsorption capacity, thermal conductivity, heat capacity and pore size were determined in a set of experimental studies. The numerical results show that thermal conductivity affects the equilibrium adsorption behavior and using materials with higher thermal conductivities yield to lower cycle time. Higher thermal

conductivity values have been obtained for new materials in comparison to silica gel. Also, pore size and diameter of the impregnated materials have been increased. On the other hand, water adsorption capacity of impregnated materials increased significantly. However, addition of metal additives decreased the adsorption rate slightly which is mainly due to the lower mass of adsorbent and higher mass transfer resistances.

**Keywords:** Solar energy, Adsorption cooling, Adsorbents, Silica gel, Impregnation, Metal additive, COMSOL Multiphysics

## ÖZ

### ADSORPSİYONLU SOĞUTMA SİSTEMLERİNDE KULLANILAN GÖZENEKLİ MALZEMELERİN ADSORPSİYON ÖZELLİKLERİ TEORİK VE DENEYSEL OLARAK İNCELENMESİ

BONYADI, NIMA

Yüksek Lisans, Makina Mühendisliği Bölümü

Tez Yöneticisi : Doç. Dr. Cemil YAMALI

Ortak Tez Yöneticisi : Doç. Dr. Derek K. BAKER

Eylül 2014 , 75 sayfa

Adsorpsiyon soğutma sistemleri, yenilenebilir enerji ile çalışabilir olmak nedeniyle dünyada daha popüler şekilde araştırılıyor. Pek çok avantajı olmasına rağmen, adsorpsiyon soğutma sistemlerinin genel verimi, buhar sıkıştırmalı soğutuculara göre hala düşüktür. Araştırmacılara göre, yatak içinde ısı ve kütle transferi ve yatağın adsorpsiyon kapasitesi, soğutma ünitesinin performansı en çok etkileyen parametrelerdir. Yatağın içinde, hem adsorpsiyon kapasitesi ve hem ısı dağıtımını artırılmasının bir yolu, emme hassasına sahip maddelerin özelliklerinin geliştirilmesi dir. Emici maddelerin adsorpsiyon özelliğini arttırmak için yeni kompozit ve karışımlar geliştirerek sağlanabilir. Emprenye yöntemi ve metal parça katkı maddeleri Kullanarak emen maddenin adsorpsiyon kapasitesi ve termal iletkenliğini artırılabilir.

Bu tez, üç ilgili çalışmanın bir bütünleşmesidir. İlk olarak, adsorpsiyon ve desorpsiyon süreçlerinde ısı iletkenlik etkisi sayısal bir model geliştirilerek incelenmiştir. Sonra, silika jel adsorbantı, metal karışımı ve emprenye yöntemlerini kullanılarak modifiye edilmiştir. Son aşamada, yeni malzemelerin su tutma kapasitesi, ısı iletkenliği, ısı kapasitesi ve gözenek boyutu gibi ısı fiziksel ve adsorpsiyon özellikleri deneysel çalışmalarla belirlenmiştir. Sayısal sonuçlara göre, ısı iletkenlik denge adsorpsiyon davranışını etkiler. Bu araştırmaya göre, daha yüksek termal iletkenliğe sahip olan malzemeler, çevrim süresini azaltmaktadır. Silika jel ile karşılaştırıldığında, yeni mal-

zemeler daha yüksek termal iletkenlik deęerleri gostermektedirler. Ayrıca, emprenye malzemelerin gözenek boyutu ve çapı artmıştır. Emprenye malzemelerin su tutma kapasitesi önemli ölçüde artmıştır. Bununla birlikte, metal parçacıkların eklenmesi, temel olarak yüzerme maddesinin daha düşük kütleyle sahip ve bu nedenle adsorpsiyon oranı küçük ölçüde azalmıştır.

Anahtar Kelimeler: Güneş Enerji, Adsorpsiyon soğutma sistemleri, Adsorbanlar, Silika gel



*To My Family*

## **ACKNOWLEDGMENTS**

I would like to express my sincere gratitude to my supervisor, Assoc. Prof. Dr. Cemil YAMALI, for his guidance, inspiration, and invaluable help all throughout the study.

I am also deeply grateful to my co-supervisor, Assoc. Prof. Dr. Derek K. BAKER, for his invaluable suggestions and guidance throughout completing my thesis work.

Besides my supervisors, I would like to thank Mustafa YALÇIN, for his technical assistance in manufacturing and conducting the experimental tests.

I furthermore wish to express my gratitude to each member of my family for providing me a comfortable and excellent environment.

This work is supported by The Scientific and Technological Research Council of Turkey (TÜBİTAK) project 113M600.

## TABLE OF CONTENTS

ABSTRACT . . . . .	v
ÖZ . . . . .	vii
ACKNOWLEDGMENTS . . . . .	x
TABLE OF CONTENTS . . . . .	xi
LIST OF TABLES . . . . .	xv
LIST OF FIGURES . . . . .	xvi
LIST OF ABBREVIATIONS . . . . .	xix
CHAPTERS	
1 INTRODUCTION . . . . .	1
1.1 Adsorption cooling cycles . . . . .	4
1.2 Enhancements in effectiveness and performance of the ad- sorbent bed . . . . .	8
1.2.1 Principle of the adsorption and desorption . . . . .	8
1.2.2 Transport in porous media . . . . .	9
1.2.3 Adsorbents and adsorbates . . . . .	10
1.2.4 Enhancements of adsorption and desorption char- acteristics of the bed . . . . .	15

	1.2.4.1	Heat transfer enhancements inside the bed . . . . .	15
	1.2.4.2	Adsorption characteristics enhancements inside the bed . . . . .	16
1.3		Survey of literature on silica gel enhancement methods . . .	17
	1.3.1	Silica gel/water investigations . . . . .	18
	1.3.1.1	Cycle and system designs . . . . .	18
	1.3.1.2	Thermo physical and adsorption properties . . . . .	19
	1.3.1.3	Modeling heat and mass transfer in porous media . . . . .	21
	1.3.2	Silica gel enhancements . . . . .	23
	1.3.2.1	Additives . . . . .	23
	1.3.2.2	Composites . . . . .	25
1.4		Objective and scope of the work . . . . .	28
2		ONE-DIMENSIONAL NUMERICAL MODELING . . . . .	31
	2.1	Introduction . . . . .	31
	2.2	Modeling procedure and fundamentals . . . . .	31
	2.3	Model description . . . . .	32
	2.4	Governing conservation equations . . . . .	33
	2.4.1	Mass conservation equation . . . . .	34
	2.4.2	Momentum conservation equation . . . . .	34
	2.4.3	Energy conservation equation . . . . .	35

2.4.4	Adsorption auxiliary equation . . . . .	35
2.4.5	Initial and boundary conditions . . . . .	37
2.5	Solution to model . . . . .	38
2.6	Results and discussions . . . . .	39
2.6.1	Base case study . . . . .	40
2.6.2	Effect of thermal conductivity of solid phase on the adsorption and desorption processes . . . . .	41
3	MATERIAL PREPARATION AND FABRICATION . . . . .	43
3.1	Introduction . . . . .	43
3.2	Silica gel preparation . . . . .	43
3.3	Enhancements in desorption characteristics . . . . .	44
3.4	Enhancements in adsorption characteristics . . . . .	45
4	EXPERIMENTAL INVESTIGATIONS ON THERMO PHYSICAL PROPERTIES OF ADSORBENTS . . . . .	49
4.1	Introduction . . . . .	49
4.2	Thermal conductivity investigation . . . . .	49
4.2.1	Thermal conductivity experimental set-up . . . . .	50
4.2.2	Test procedure . . . . .	51
4.2.3	Result and discussions . . . . .	51
4.2.4	Effective thermal conductivity model . . . . .	53
4.3	BET analysis . . . . .	54
4.4	Heat capacity analysis . . . . .	56

5	INVESTIGATING THE INFLUENCE OF MODIFICATIONS ON THE PERFORMANCE OF AN ADSORPTION COOLING UNIT . .	59
5.1	Introduction . . . . .	59
5.2	Description of the experimental set-up and components . . .	59
5.2.1	Adsorbent bed . . . . .	60
5.2.2	Evaporator/Condenser . . . . .	61
5.2.3	Water bath and oven . . . . .	62
5.2.4	Piping system . . . . .	62
5.2.5	Measurement devices . . . . .	63
5.3	Experimental procedure . . . . .	64
5.4	Result and discussions . . . . .	65
6	CONCLUSIONS AND RECOMMENDATIONS . . . . .	69
	REFERENCES . . . . .	71
	APPENDICES	

## LIST OF TABLES

### TABLES

Table 1.1	Cycle Performance of commonly used working pairs [1]. . . . .	15
Table 1.2	The performance and working conditions for different working pairs [2]. . . . .	27
Table 2.1	Model parameters [3]. . . . .	38
Table 3.1	The thermo physical properties of silica gel [3]. . . . .	44
Table 3.2	Thermo physical properties of aluminum metal chips. . . . .	45
Table 3.3	An overview of different experimental investigations and tested materials. . . . .	48
Table 4.1	Specifications of the conductivity set-up. . . . .	51
Table 4.2	Experimental data and obtained results for the thermal conductivity measurements. . . . .	52
Table 4.3	The results for experimental and theoretical investigations on mixture thermal conductivity. . . . .	54
Table 4.4	BET test results for samples. . . . .	55

## LIST OF FIGURES

### FIGURES

Figure 1.1	Worldwide energy consumption projections in 2040 [4]. . . . .	1
Figure 1.2	Energy consumption in residential sector in US [4]. . . . .	2
Figure 1.3	COP values of sorption cooling systems with driving temperatures [5]. . . . .	3
Figure 1.4	The schematic of a basic adsorption cooling cycle. . . . .	5
Figure 1.5	Clapyron diagram of the cycle of a basic adsorption cooling cycle [1]. . . . .	6
Figure 1.6	Working principle of a thermal wave cycle [1]. . . . .	7
Figure 1.7	Transport, Reaction and Phase Change in Porous Media [6]. . . . .	10
Figure 1.8	array of $\text{SiO}_4$ in silica gel [7]. . . . .	13
Figure 1.9	Crystal cell unit of zeolite: (a) crystal cell unit of type A zeolite; (b) crystal cell unit of type X, Y zeolite [7]. . . . .	14
Figure 1.10	Structure of activated carbon [7]. . . . .	14
Figure 1.11	The schematic view of the thermal conductivity experimental set- up [8]. . . . .	20
Figure 1.12	Thermal conductivity of a dry silica gel bed as a function of the air pressure (Pa) [8]. . . . .	20
Figure 1.13	Differential element for a one-dimensional GSSR model [9]. . . . .	22
Figure 1.14	Temperature differences between the solid and gas phases in one- dimensional transient modeling [3]. . . . .	23
Figure 1.15	metal chips: a) copper; b) aluminum; c) stainless steel; d) brass [10].	24
Figure 1.16	COP comparison for different working pairs [2]. . . . .	27
Figure 1.17	Driving temperature comparison for different working pairs [2]. . .	28



Figure 2.1	Schematic view of the cylindrical adsorbent bed. . . . .	32
Figure 2.2	Two phase flow illustration in representative elementary volume [11].	33
Figure 2.3	Modeling domain with boundary conditions. . . . .	37
Figure 2.4	Schematic view of the one-dimensional symmetrical model in COM-SOL Multiphysics. The points 1 to 6 are at 65 mm, 55 mm, 45 mm, 35 mm, 25 mm and 15 mm distance from the cylinder wall, respectively. . . .	39
Figure 2.5	Temperature distribution during adsorption process inside the bed. .	40
Figure 2.6	Water uptake amount during adsorption process inside the bed. . .	40
Figure 2.7	Temperature distribution during desorption process inside the bed. .	41
Figure 2.8	Temperature distribution during adsorption process for different thermal conductivity values. . . . .	42
Figure 2.9	Water uptake amount during adsorption process for different thermal conductivity values. . . . .	42
Figure 2.10	Temperature distribution during desorption process for different thermal conductivity values. . . . .	42
Figure 3.1	Picture of the supplied silica gel granules. . . . .	44
Figure 3.2	Picture of the prepared aluminum metal additive. . . . .	45
Figure 3.3	Picture of the supplied calcium chloride. . . . .	46
Figure 3.4	The picture of (a) final impregnated silica gel; (b) unmodified silica gel. . . . .	47
Figure 4.1	Thermal conductivity test set-up. . . . .	50
Figure 4.2	Picture of the conductivity test facility. . . . .	50
Figure 4.3	The variations of results for thermal conductivity of the samples with temperature. . . . .	53
Figure 4.4	The experimental and theoretical thermal conductivity results for different volume proportions of aluminum. . . . .	54
Figure 4.5	Pore width of the samples. . . . .	55
Figure 4.6	Pore diameter of the samples. . . . .	55
Figure 4.7	Surface area of the samples. . . . .	56

Figure 4.8 Heat capacity variations of pure silica gel with time. . . . .	56
Figure 4.9 Heat capacity variations of S20 with time. . . . .	57
Figure 4.10 Heat capacity variations of S40 with time. . . . .	57
Figure 4.11 Heat capacity distribution of S60 with time. . . . .	57
Figure 5.1 A schematic view of the experimental set-up (C-1 Oven; C-2 Adsorbent bed; C-3 Adsorbent bed thermocouple output; C-4 Vacuum pump; C-5 Pipe thermocouple output; C-6 Evaporator thermocouple output; C-7 Water bath; C-8 Evaporator/Condenser; C-9 V-C cooling system; C-10 Electrical heater; C-11 Circulation pump; V-1 ... 5 Vacuum valves; P-1,2 Pressure transducers). . . . .	60
Figure 5.2 The outer and inner view of the adsorbent bed and its components. .	60
Figure 5.3 The photograph of the evaporator/condenser component used in the system. . . . .	61
Figure 5.4 The photograph of the water bath and oven used in the system. . .	62
Figure 5.5 The photograph of the rotary vacuum pump used in the system. . .	62
Figure 5.6 The photograph of thermocouple feedthroughs in the left and pressure transducer in the right. . . . .	63
Figure 5.7 The photograph of the DAQ system. . . . .	63
Figure 5.8 Temperature and pressure distribution in adsorption process for silica gel. . . . .	65
Figure 5.9 Temperature and pressure distribution in adsorption process for S40.	65
Figure 5.10 Temperature and pressure distribution in adsorption for Si-10% Al.	66
Figure 5.11 Water uptake distribution in adsorption process for silica gel. . . .	66
Figure 5.12 Water uptake distribution in adsorption process for S40. . . . .	67
Figure 5.13 Water uptake distribution in adsorption process for Si-10% Al. . . .	67

## LIST OF ABBREVIATIONS

### Symbols

$A$	area, $\text{m}^2$
$COP$	coefficient of performance
$c_p$	heat capacity, $\text{Jkg}^{-1}\text{K}^{-1}$
$D_e$	equivalent diffusivity in the adsorbent particles, $\text{m}^2\text{s}^{-1}$
$d_p$	diameter of the adsorbent particle, m
$d_{pore}$	average pore diameter, m
$E_a$	activation energy of surface diffusion, $\text{kJkg}^{-1}$
$k_m$	mass transfer coefficient within the adsorbent particles, $\text{s}^{-1}$
$k$	thermal conductivity, $\text{Wm}^{-1}\text{K}^{-1}$
$P$	pressure, kPa
$Q$	energy, kJ
$Q_{ad}$	isosteric heat of adsorption, $\text{kJkg}^{-1}$
$R_g$	specific gas constant for water, $\text{kJkg}^{-1}\text{K}^{-1}$
$r$	Radial coordinate, m
$T$	temperature, K
$t$	time, s
$V$	volume, $\text{m}^3$
$v$	velocity, $\text{ms}^{-1}$
$v_r$	gas phase velocity in radial direction, $\text{ms}^{-1}$
$X$	amount adsorbed or adsorption capacity, $\text{kg}_w\text{kg}_s^{-1}$
$z$	axial coordinate, m

### Greek symbols

$\mu$	viscosity
-------	-----------

$\rho$	density, $\text{kgm}^{-3}$
$\epsilon$	volume fraction
$\epsilon_t$	total porosity
$\epsilon_b$	bed porosity
$\epsilon_p$	particle porosity
$k_{ge}$	effective thermal conductivity for the gas phase, $\text{Wm}^{-1}\text{K}^{-1}$
$k_{se}$	effective thermal conductivity for the solid phase, $\text{Wm}^{-1}\text{K}^{-1}$
$k_{le}$	effective thermal conductivity for the liquid phase, $\text{Wm}^{-1}\text{K}^{-1}$

## Subscripts

ad	adsorbent
b	boundary
g	adsorbate gas
l	liquid
s	solid adsorbent
v	vapor
ev	evaporator
sat	saturation
con	condenser
$\infty$	infinity
$i$	input

# CHAPTER 1

## INTRODUCTION

Energy has the dominant role in the world economy policy which is highly related to well-being and prosperity of the people. Statistics show that there is a growing demand for energy due to the population growth around the globe. Figure 1.1 shows the increasing energy consumption and the projections through 2040 worldwide [4]. As shown in this figure, despite increasing trend of renewable energy application, fossil fuels will still supply most of the energy consumption in the future. Higher energy usage through burning carbon based fossil fuels such as liquids, coal and natural gas leads to the production of more greenhouse gases like carbon dioxide ( $\text{CO}_2$ ) which will be released to the atmosphere and consequently causes climate change and global warming. Therefore, finding a solution for meeting the growing demand for energy in a safe and environmentally benign manner is one of the main challenges in front of the nations. Currently, renewables have a small share of the world energy supply but energy crisis and diminishing fossil fuels speed up the renewables industry growth globally.

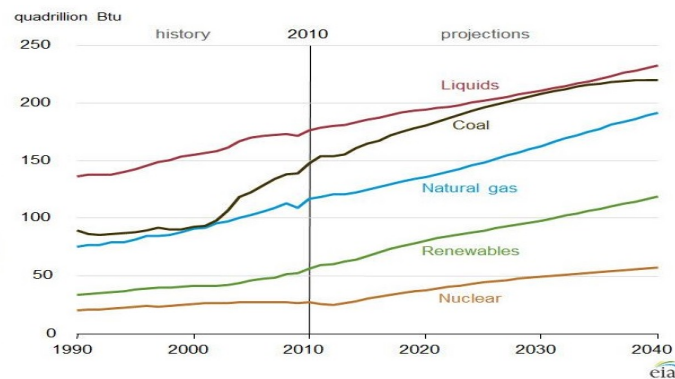


Figure 1.1: Worldwide energy consumption projections in 2040 [4].

Figure 1.2 shows the total energy consumption of the residential sector in US [4]. From this figure, an increase in electricity consumption on the hottest months and very large increment of natural gas usage during the coldest months of the year can be inferred. These increasing trends are mainly due to the higher application of cooling and heating systems, respectively. On the other hand, the International Institute of Refrigeration (IIR) has reported that energy supply to refrigeration and air-conditioning systems of different kinds constitutes approximately 15% of all electricity produced worldwide [2]. This ratio would be rapidly increasing with improvement of living level especially in countries with hot and humid climate. Therefore, developing the conventional air conditioning systems in a way to be applicable with renewables like solar energy or waste heat is of great importance. One instance of such systems that can be driven with renewables is thermally driven sorption cooling systems.

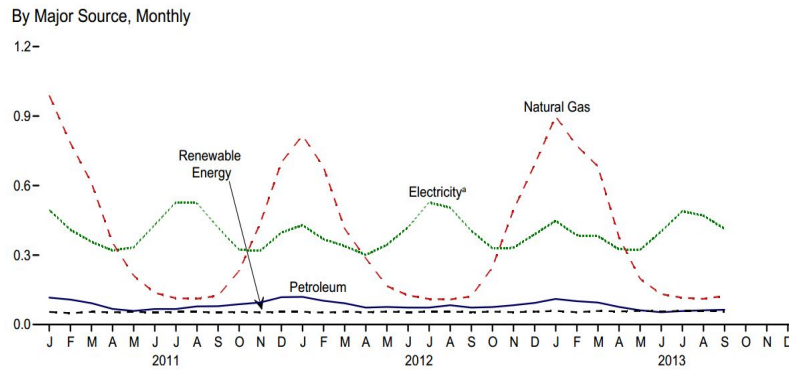


Figure 1.2: Energy consumption in residential sector in US [4].

Vapor compression cooling systems (VCS) consume large amounts of electrical energy, typically produced by burning fossil fuels. One effective way to meet cooling loads with lower cost and pollution is to replace conventional electrically-driven systems with environmentally benign, low grade thermal-powered sorption cooling systems. Sorption technology is classified as closed cycle and open cycle sorption systems. Closed cycle sorption technology is also divided into solid sorption (adsorption) and liquid sorption (absorption) refrigeration. The absorption is a physical or chemical process in which atoms, molecules, or ions enter some bulk phase of a solid, liquid or gas material. In contrast, adsorption is a surface phenomenon and the adsorbate is mostly concentrated on the surface of the adsorbent material. On the other hand, open cycle solid sorption, termed as desiccant systems, are mainly dealing with the latent load of the air. Solid sorption cooling technologies are not yet

competitive with conventional electricity-driven air-conditioners due to their high investment costs and low coefficient of performance (COP) and specific cooling power (SCP). Figure 1.3 represents the COP values of sorption cooling systems in different driving temperatures [5]. According to this figure, absorption technology has the highest COP range but on the other hand, adsorption cooling technology is capable of working with lower driving temperature.

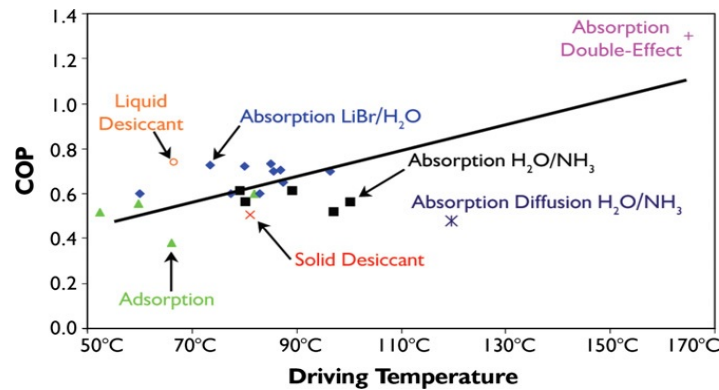


Figure 1.3: COP values of sorption cooling systems with driving temperatures [5].

Despite lower performance, longer cycle time and higher cost of adsorption cooling systems, the following items are the main advantages of adsorption technology over vapor compression and absorption cooling systems [1, 12]:

- Compatibility to work with lower driving temperature energy sources which accommodate the application of flat plate solar collectors;
- Operating without noise and vibration;
- Do not require frequent maintenance;
- Longer life time;
- Environmentally friendly;
- Applicable in remote areas;
- Possibility to work with high temperature heat sources without corrosion;
- Simpler to design in comparison to other systems
- More suitable for small systems.

Adsorption technology was first introduced by Faraday in 1848 but its application in heat pumps and refrigeration was started in 1920s [13]. Solid sorption cooling systems are feasible in all ambient conditions but especially more economical in climates with hot and long summers such as mediterranean region. Both open and closed solid sorption systems have two main components for producing the desired air conditioning, namely adsorbent bed or dehumidifier and regeneration heat source. Closed cycle solid sorption cooling systems which are shortly called as adsorption cooling systems (ADS) have some other components for completing the refrigeration cycle such as condenser, evaporator and expansion valve. ADS cycle and vapor compression cycle are similar to each other. The only difference is the replacement of electrically-driven compressor by thermally-driven adsorbent bed. In desiccant systems, the latent and sensible loads are separately processed in dehumidifier and cooling unit, respectively, i.e. the moisture of the air is removed in dehumidifier and temperature is controlled inside the cooling unit. Separate processing decreases energy consumption in comparison to other heat pumps since cooling-based dehumidification systems consume more energy to decrease humidity only by reducing the temperature in one process [14]. Adsorption systems are mainly used for air conditioning and ice-making purposes but desiccant systems are widely applied for air conditioning, moisture removal and filtrations. Solid sorbents like silica gel is used in both systems which is selected based on the aim of the application. While the main focus of this study is on adsorption cooling systems, the results are applicable to both adsorption and desiccant systems.

## **1.1 Adsorption cooling cycles**

The schematic of a basic adsorption cooling cycle and Clapyron diagram of the cycle are shown in Figure 1.4 and Figure 1.5, respectively. The major components that produce the desired air conditioning in a basic adsorption cooling systems are adsorbent bed, regeneration heat source, evaporator, condenser and expansion valve.

As illustrated in Figure 1.5, the cycle begins at point 1 as the oil which is heated by solar energy or waste heat, is used to increase the temperature of the bed. This process continues until the adsorbent pressure reaches to the condenser pressure. In process



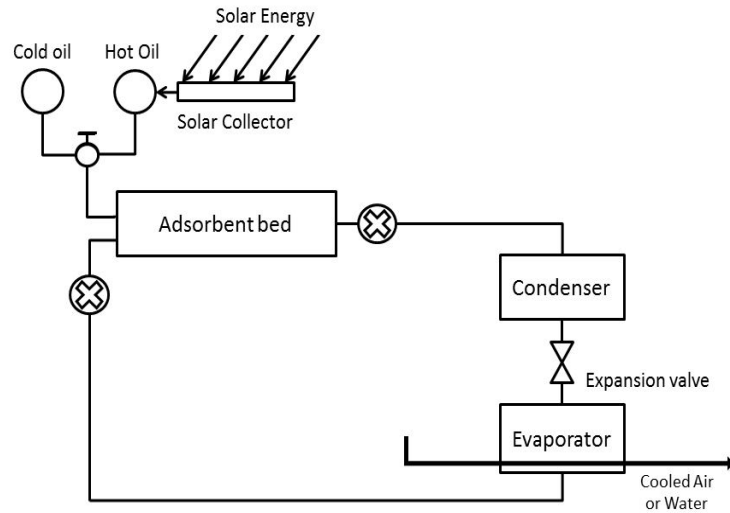


Figure 1.4: The schematic of a basic adsorption cooling cycle.

2-3, the bed is still heated from the outside and desorption process starts. The refrigerant emanates from the bed in gas phase and enters the condenser to get condensed and changes to liquid completely. At point 3, the desorption process ends and the bed is cooled down in process 3-4. The condensed liquid is expanded to the desired evaporator pressure by passing through the expansion valve. As the temperature and pressure inside the bed decreases, adsorption process starts when pressure reaches to the evaporator pressure at point 4. The cycle ends in the process 4-1, while the refrigerant inside the evaporator is vaporized taking the heat from the air or water that is aimed to get cooled. The adsorption process continues until the system reaches a steady state condition and no more adsorption takes place. After reaching equilibrium condition and no more adsorption occurs, the cycle restarts by taking heat in process 1-2. Importantly, based on the refrigerant characteristics, different working conditions should be maintained in different parts of the system. For instance, if water is used as refrigerant, the pressure should be kept under the saturation pressure of water at evaporator temperature. Therefore, the system should be vacuumed properly. Also, based on the required driving temperature for the desorption process, different types of solar collectors such as air, flat plate and evacuated tube can be utilized [12].

COP and SCP are two main parameters that express the efficiency and effectiveness of a cooling unit, respectively. The COP is a measurement of the energy efficiency of air conditioners and is defined as the ratio of useful work or energy output to the

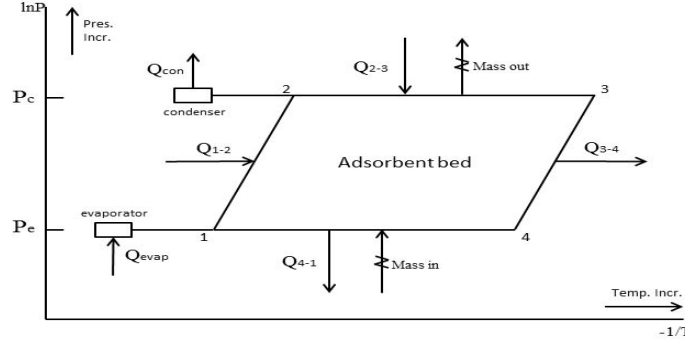


Figure 1.5: Clapyron diagram of the cycle of a basic adsorption cooling cycle [1].

amount of work or energy input. In the basic adsorption cycle, COP is expressed as:

$$COP = \frac{Q_{ev}}{Q_{1-2} + Q_{2-3}} \quad (1.1)$$

SCP is another expression which is expressed as the cooling per cycle divided by mass of the adsorbent and cycle time.

$$SCP = \frac{Q_{ev}}{mt_{cycle}} \quad (1.2)$$

Since the adsorption bed operates intermittently, therefore different cycles with two or more beds are required to meet the cooling demands continuously. Moreover, in order to increase the efficiency, several cycles have been developed in recent years which consume lower energy and obtain higher COP values in comparison to basic adsorption systems. These cycles can be classified into heat and mass recovery, thermal wave and multi-bed and multi-stage cycles .

**Heat and mass recovery cycles:** In this cycle, adsorption and desorption processes occur simultaneously in two or more separate beds. This feature makes the system run continuously. The other advantage of heat recovery cycles, is using the rejected heat from adsorption process of one bed in desorption process of the other. Some researchers have developed heat recovery cycles and reported large amount of energy recovery leading to higher COP values in comparison to basic cycles [15, 16]. The

COP value in heat recovery cycles is calculated by the following equation:

$$COP = \frac{Q_{ev}}{Q_{1-2} + Q_{2-3} - Q_{reg}} \quad (1.3)$$

In some studies, mass recovery is also employed in addition to heat recovery process. Mass recovery can be applied by simply transferring refrigerant vapor between the beds. This connection brings about the refrigerant flows from the higher pressure bed which has the higher temperature to the bed with lower pressure and temperature [17, 18].

**Thermal wave cycle:** Thermal wave cycle is the combination of two adsorbent beds, one heater, one heat exchanger together with one or two circulating pumps. In this cycle, heat is given to the cold bed by the heat transfer fluid which receives the heat from the hot bed using the heat exchanger. Therefore, the amount of heat rejected to ambient is decreased significantly [19]. In a study conducted by Zhang et al. [20], the effects of operating parameters on the effectiveness of a thermal wave system was investigated. They reported an increase on COP and cooling capacity by 20% and 50%, respectively. Thermal wave cycles are only applicable to single stage cycle, which are not efficient and effective at very low and high temperatures. Therefore, other studies have been performed on different types of advanced cycles with the aim of increasing the COP and SCP of adsorption cooling units. The working principle of a thermal wave cycle is shown in Figure 1.6 [1].

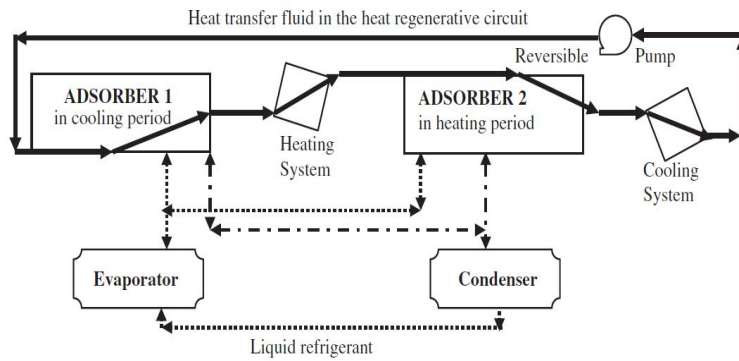


Figure 1.6: Working principle of a thermal wave cycle [1].

**Multi-bed and multi-stage cycle:** By applying heat and mass recovery to multi-bed and multi-stage configurations, better performances can be achieved with some mod-

ifications and the effectiveness of the system increases significantly [21]. Khan et al developed a heat and mass recovery cycle with the concept of multi-stage configuration and has reported very low regenerating temperature with optimum cooling capacity [22].

## **1.2 Enhancements in effectiveness and performance of the adsorbent bed**

In adsorption cooling cycle, the component which highly affects the performance of the system is the adsorbent bed. The process of adsorption and desorption takes place inside the bed chamber which is filled with solid adsorbent materials. Based on the adsorbent and adsorbate working pairs the system works at vacuum conditions in some cycles. Therefore, the bed should be designed and fabricated accordingly to maintain the required pressure. Moreover, since adsorption and desorption phenomenon occur inside the bed, the concept behind materials adsorption and heat and mass transfer of refrigerant should be investigated completely.

### **1.2.1 Principle of the adsorption and desorption**

Adsorption is defined as the separation of a substance from one phase and its concentration at the surface of another material. The adsorption phenomenon is applied widely in moisture removal systems, catalysts, separation of gases, purification of liquids and pollution control. The adsorbing phase is called the adsorbent and the adsorbed material at the surface of the adsorbent is called adsorbate [23]. Generally, the two forms sorption that exist are physical and chemical. In physical sorption technology, the adsorbate molecules form a van der Waals bonding with surface molecules which requires very low heat to break this bond and therefore the adsorption process in this form is easily reversible. Hence, adsorbent and adsorbate working pairs are widely used in low grade thermal cooling systems [13]. The most common physical working pairs used in adsorption refrigeration technology are silica gel/water, zeolite/water, activated carbon/methanol and activated carbon/ammonia. On the other hand, chemical sorption is caused by the electron transfer, atom rearrangement and fracture or formation of chemical bond and only one layer of sorbate

reacts with the surface molecules of chemical sorbent. In chemisorption, the sorbent and sorbate molecules never stay in their original state after the sorption process [21]. Chemisorption materials mainly include metal oxides, metal chlorides and metal hydrides. Among all chemical sorbents, calcium chloride is widely used for adsorption refrigeration. One drawback of metal chlorides is salt swelling and agglomeration during the absorption process which impact the heat and mass transfer performances.

Generally, adsorption phenomenon is an exothermic process and heat is released to the surroundings as the adsorbates are adsorbed on the surface of materials. Heat of adsorption causes temperature rise through the adsorbent bed which affects the performance of the adsorbents [24].

Desorption is defined as the regenerating process of the adsorbents and removing the adsorbate from the surface of materials to continuously iterate the cooling cycle. Lower regeneration temperature of adsorbents means lower energy requirements and consequently higher performance of the system. Desorption is usually performed by heating the adsorbents. Solar energy or waste heat is usually chosen as the heat source. The efforts are in progress to lower the values of regenerating temperature and increase the potential of utilizing solar energy [25]. Adsorption capacity of adsorbents and rate of heat and mass transfer within the adsorbent bed are two important factors affecting the performance of adsorption and desorption processes. These parameters are investigated in the following sections.

### **1.2.2 Transport in porous media**

A porous medium is made of a solid matrix with interconnected voids. Fluids can flow through the porous material using the voids in single-phase flow (i.e. single fluid) and two-phase flow (i.e. a liquid and a gas). The porosity and permeability are two commonly used parameters to characterize a porous medium. Mass transfer resistances for adsorbate gas flow are determined by permeability through the void between the solid sorbent particles. The porosity is expressed as the proportion of the void space to the total volume of the medium. Due to the nature of the porous media, the definition of the porosity also covers the void spaces within the particles which are called particle porosity or intra-particle porosity [6, 3].

Transport of mass, momentum and energy, chemical reactions and phase change in porous medium are indicated in Figure 1.7. The above phenomenon can be described in two forms of micro-scale at the level of the inter-spaces within the adsorbents and a macro-scale. On the microscopic scale, the flow quantities like velocity and pressure will be clearly irregular. These quantities can be measured over areas that cross many pores by using the volume averaging theory. Such space-averaged quantities change in a regular manner with respect to space and time in a relatively accurate and yet solvable description. Hence, theoretical simulations can be applied by combining the two scales in a simplified form [26]. This method has been applied widely for transport analysis in porous media. In this approach, a macroscopic variable is defined as an appropriate mean over a sufficiently large representative elementary volume (REV). The size of the REV is assumed to be greater than the individual adsorbent particles and smaller than the overall system dimensions [27]. The governing equations describing the heat and mass transfer and adsorption processes inside the adsorbent bed are then developed and solved numerically. More information about simulations are given in the next sections.

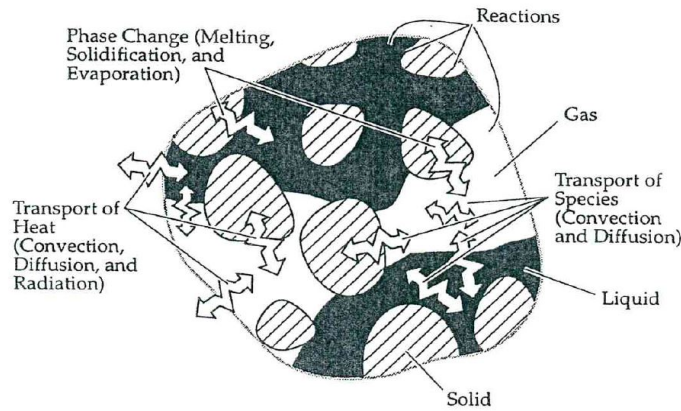


Figure 1.7: Transport, Reaction and Phase Change in Porous Media [6].

### 1.2.3 Adsorbents and adsorbates

The adsorption is a surface phenomenon and the performance of adsorption depends on surface properties, such as surface area, polarity, micropores and macro-pores, size of granules and crystals. Hence, microporous adsorbents with pore diameters ranging from a few Angstroms to a few tens of Angstroms are chosen as adsorbents

to obtain adequate adsorptive capacity. Adsorbents are classified into traditional microporous adsorbents like silica gel and recently developed materials such as zeolites. The micropore diameter and the width of the distribution can be controlled by the manufacturing process in traditional adsorbents. However, the size of the pores in zeolites are controlled by crystal structure without any distribution of pore size [6]. In another classification, the adsorbents are divided into physical and chemical sorption materials. Common physisorption adsorbents used in adsorption cooling cycles are Silica gel, zeolites and activated carbon. The chemical working pairs which are frequently used in adsorption cooling cycles are metal chloride/ammonia, metal hydrides and hydrogen and metal oxides and oxygen.

Water, ammonia and methanol, known as widely used refrigerants, have relatively high latent heats of 2258, 1368 and 1160 kJ/kg, respectively. Ammonia is a corrosive material and methanol is flammable. Water is thermally stable in the presence of suitable adsorbents. The disadvantage of water is that it cannot be used for freezing and ice-making applications because of its freezing temperature at 0 °C [28].

Adsorbent and adsorbate working pairs should be selected correctly to have the optimal performance of the system. For instance, 'hydrophilic' adsorbents have special affinity with polar materials like water. Silica gel, zeolites and active alumina are in this category. On the other hand, some adsorbents have more affinity for non-polar substances which are termed as 'hydrophobic' like activated carbons and polymer adsorbents. Ideal adsorbents should possess the following characteristics:

- A large adsorptive capacity;
- Suitable thermal properties like high conductivity and diffusivity and low specific heat capacity;
- Regeneration at low driving temperatures;
- Excellent compatibility with the refrigerant;
- Availability and low cost;
- High durability.

Ideal conditions and characteristics of adsorbates are as follows [13, 3]:

- Desired evaporation temperature and pressure;
- Good latent heat capacity;
- Non-flammable;
- Good thermal stability;
- Low specific heat;
- Compatibility with the adsorbent;
- Non-corrosive, etc.

### **Silica gel**

Silica gel is made from silicon dioxide hydrosol after sequentially undergoing the process of condensation, polymerization, aging and being partially dehydrated [29]. The chemical composition of silica gel is  $\text{SiO}_2 \cdot n\text{H}_2\text{O}$  and the water content which is present mainly in the form of chemically bond hydroxyl groups, amounts typically to about 4-6 wt.%. This amount of water cannot be removed, otherwise the silica gel would lose the adsorption capability. Thus, silica gel should not be heated to temperatures higher than 120 °C, and it is generally regenerated at lower than 90 °C. Hydroxyl groups causes a degree of polarity to the surface so that water molecules are adsorbed on the surface of silica gel. One hydroxyl can adsorb one molecule of water and polarization of the hydroxyl ions greatly impact the COP of silica gel adsorption systems. Silica gel is regenerated at low temperatures which brings about the possibility to be utilized in low grade thermal adsorption cooling systems. Due to the physical adsorption of water vapor into its internal pores, silica gel faces no chemical reaction and shape change even after saturation with water vapor. However, the pair cannot produce cooling below 0 °C [7]. Figure 1.8 shows the array of  $\text{SiO}_4$  in silica gel.

Silica gel was first used during the First World War in gas masks but the most important current application of silica gel is as a desiccant. There are two types of silica gel produced with pore diameters of 2-3 nm (A type) and 0.7 nm (B type).



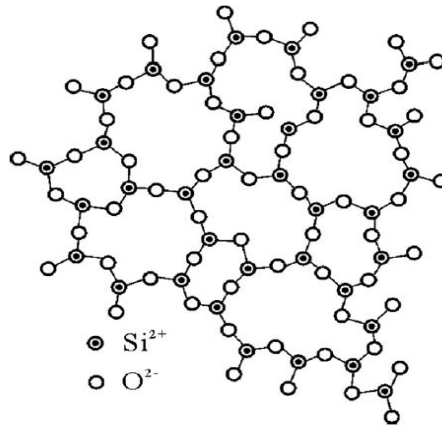


Figure 1.8: array of  $\text{SiO}_4$  in silica gel [7].

## Zeolites

Zeolites are porous crystalline aluminosilicates. The framework of zeolite is a collection of  $\text{SiO}_4$  and  $\text{AlO}_4$  tetrahedra which forms an open crystal lattice containing pores of molecular dimensions into which adsorbate molecules can penetrate. There are about 40 types of natural zeolites and 150 types of artificially synthesized frameworks which are named by one letter or a group of letters, such as type A, type X, type Y, type ZSM, etc [6]. Artificially synthesized zeolites are more expensive than natural zeolites, but they have higher bulk specific weight and better heat transfer characteristics. Different refrigerants are selected based on the pore size of zeolites. One crystal unit of zeolite is shown in Figure 1.9. This crystal is capable to maintain 235 molecules of water after adsorption [7]. Zeolites can also be utilized in both desiccant cooling system and adsorption refrigeration system. However, due to the low working pressure, mass transfer performance of the pair is weak. Also, high values of adsorption heat and desorption temperature, increases the cycle time and requires a heat source to provide higher temperature.

## Activated carbon

Activated carbon is manufactured by thermal decomposition of carbonaceous materials followed by activation by steam or carbon dioxide at elevated temperature. The surface of activated carbon is non-polar. As a result, carbon adsorbents tend to be hydrophobic. Therefore, they are widely used for water purification, solvent recovery systems and air purification systems. The adsorption processes of activated carbon

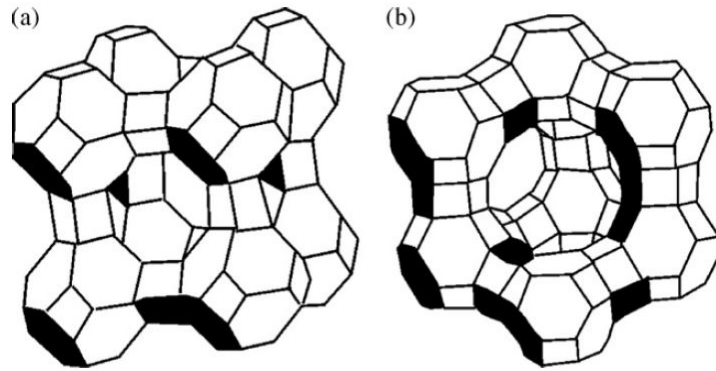


Figure 1.9: Crystal cell unit of zeolite: (a) crystal cell unit of type A zeolite; (b) crystal cell unit of type X, Y zeolite [7].

and methanol working pair occurs in micropores, which has specific area between 500 and 1500 m<sup>2</sup>/g. Activated carbon and methanol is one of the most common working pair due to the large adsorption quantity and lower adsorption heat, which is about 1800–2000 kJ/kg [7]. Activated carbon and methanol is also a suitable working pair to use solar energy as heat source due to the low desorption temperature and can be used for refrigeration purpose at sub-zero temperature. However, latent heat of vaporisation for methanol is only half of that for water [5]. The structure of activated carbon is illustrated in Figure 1.10.

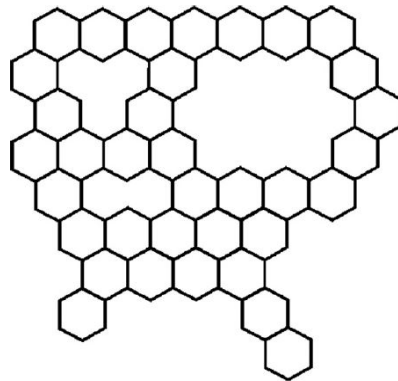


Figure 1.10: Structure of activated carbon [7].

Among all the above adsorbents, silica gel possesses the characteristics which are suitable for both air conditioning and moisture removal applications. All adsorbents and adsorbates have advantages and disadvantages and the appropriate working pair should be selected based on the application. However, as illustrated in Table 1.1, silica gel/water working pair seems more appropriate to be used in low grade thermal

adsorption cycles due to lower regeneration temperature requirements and compatibility with water vapor.

Table 1.1: Cycle Performance of commonly used working pairs [1].

Adsorbents	Max adsorbate capacity ( $\text{kg}_w \text{ kg}_s^{-1}$ )	COP range	Reg. temp $^{\circ}\text{C}$	Min evaporation temp $^{\circ}\text{C}$
Silica gel	0.37	0.25 - 0.65	60 - 100	Can not be less than zero
zeolites	0.3	0.28 - 1.4	150 - 300	Can not be less than zero
Activated carbon	0.32	0.12 - 1.06	100	Can work in lower temperature to $-97^{\circ}\text{C}$

#### 1.2.4 Enhancements of adsorption and desorption characteristics of the bed

Poor heat transfer rate in the adsorbent bed is caused mainly due to low thermal contact between the bed and the adsorbent and low thermal conductivity and high porosity of the adsorbents. Also, geometry and shape of the bed are other important parameters influencing the heat and mass transfer rate. On the other hand, conventional adsorbents have low water uptake capability and high mass transfer resistances which in overall decrease the adsorption capacity of the bed. There are some methods that have been widely used for decreasing heat and mass transfer resistances and incrementing the adsorption capacity.

##### 1.2.4.1 Heat transfer enhancements inside the bed

Heat transfer enhancements includes both bed modifications and material improvements which can be performed by a variety of methods.

**Extended surfaces:** Increasing the heat transfer area is the aim of using this method. Applying fins inside the heat exchangers [30] is one way to increase the contact surface area. For optimizing the design of the bed, constructal (tree-network) theory can be used for designing the bed with enhances the heat and mass transfer properties. For detailed information about this theory, refer to [3, 31].

**Coated beds:** In this process, adsorbents are adhered to the inner surface of the

adsorbent bed. Coating the bed with adsorbents decreases the heat transfer resistances and therefore increases the wall heat transfer coefficient. Coatings are applied using a variety of methods such as spray, coil and curtain coatings. In an experimental study performed by Restuccia et al [32], the finned tubes inside the adsorbent bed are coated with a layer of zeolite. The results show a specific cooling power of 30–60  $\text{Wkg}^{-1}$  and a cycle time of 15–20 min based on different working conditions. They have concluded that coating the bed produces better results in comparison to those measured without coating. Some other experimental studies have been performed to investigate the performance of coated beds in the literature [32, 33, 34].

**Additives:** Adding materials with high thermal conductivity like aluminum and copper chips can significantly improve thermal conductivity and diffusivity of the adsorbents without changing the adsorption capacity. In a simple mixture, the adsorbent and the additive are simply mixed with the desired mass or volume ratio. Generally, the aim of this method is to produce a material which increases heat transfer to a satisfactory level. The only disadvantage of this method is resulting lower mass transfer rate due to increment of resistances caused by the metal pieces. The commonly used additives are metallic chips, metal powders, expanded graphite, activated carbon and carbon fibres. Additives like expanded graphite and activated carbon improve the permeability and mass transfer characteristics in addition to their good thermal conductivity [10, 35].

#### **1.2.4.2 Adsorption characteristics enhancements inside the bed**

Despite many superior characteristics, adsorbents like silica gel have some disadvantages. Low adsorption capacity and thermal conductivity of this adsorbent causes lower efficiency and longer cycle time in an adsorption cooling cycle. In this regard, some methods have been advised by researchers to overcome these problems and improve the characteristics of adsorbents. Several theoretical and experimental studies have also been conducted to evaluate the impact of these methods. Heat and mass transfer enhancements and increasing water uptake capacity of adsorbents are the main objectives of these studies. These methods are performed by constructing composite materials which combines the physical and chemical adsorbents. According

to the literature, impregnating and consolidating are two methods that raise adsorption capacity of adsorbents. Wang et al [7] declare that the composite adsorbents are usually made from porous media and chemical sorbents. Impregnated adsorbents are produced by dissolving the chemical adsorbent in the distilled water or the solvent and then putting the additive in the solution and finally drying it to remove the solvent. Consolidated adsorbent is made by compressing the powder prepared from the first method. Each of these enhancement methods causes different characteristics in final products. The impregnation method produces large porosity inside the media which causes mass transfer enhancement and consolidated adsorbents show higher thermal conductivity but a large number of operations are necessary to fabricate the compound [12]. The main shortcoming of consolidated adsorbents is that by increasing heat transfer in adsorbents, there is a reduction in mass transfer performance. Therefore, enhancing the mass transfer by methods such as creating voids in the bed is important [3]. Most commonly investigated advanced working pairs are silica gel and chlorides/water, silica gel and chlorides/methanol, chlorides and porous media/ammonia and zeolite and foam aluminum/water [2].

### **1.3 Survey of literature on silica gel enhancement methods**

Working pairs exert a strong influence adsorption and desorption processes in the adsorbent bed. Among the commercially used working pairs, silica gel and water demonstrate high adsorbing and desorbing quality. Investigations have been performed in the literature to determine the properties of silica gel/water and evaluate the performance of the working pair in an adsorption cooling unit. However, like any other adsorbent, the performance of silica gel can be further enhanced. There are modification methods in which the properties of silica gel are changed significantly when the granules pass through some processes. These methods are mainly aimed to improve the heat transfer rate and adsorptivity of the adsorbent. The following is a review of the recently conducted experimental and theoretical studies on the silica gel enhancement methods. This section contains comparative information about silica gel adsorption systems based on the important cycle parameters like COP, SCP, driving temperature and evaporation temperature.

### 1.3.1 Silica gel/water investigations

Silica gel/water is the earliest working pair used commercially in adsorption refrigeration systems. In the past few decades, more attention has been given to silica gel/water working pair, especially in air conditioning facilities. Due to specific characteristics like high affinity for water, silica gel is still widely used as desiccant in moisture removal technology and desiccant cooling systems. Generally, the investigations of silica gel/water adsorption systems include cycle and system designs, determining thermo physical and adsorption properties and theoretical modeling.

#### 1.3.1.1 Cycle and system designs

Some researchers have developed adsorption cooling cycles in which silica gel is used as the adsorbent. The aim of these studies is to evaluate the performance of different experimental systems. In a silica gel adsorption chiller fabricated by Shanghai Jiaohong University in Japan, the driving temperature is reported as 55 °C which accommodates the application of flat plate solar collectors [36, 37]. The performance of a novel silica gel/water adsorption chiller was tested in an experimental study conducted by Wang et al [36]. The results show that the SCP and COP of the system are 126 W kg<sup>-1</sup> and 0.38, respectively. A conclusion from these studies is that this system can be effectively driven by low-grade heat source like solar energy.

In addition to basic configurations, cycles with heat and mass recovery and multi-bed, multi-stage systems have been also investigated with adsorbent silica. In a study [38], Lu et al has developed a solar adsorption chiller with heat and mass recovery cycle in which 65 kg of silica gel was put inside each bed. The influence of operating conditions on the performance of chiller was investigated. The system possesses a COP and SCP values of 0.63 and 275 W kg<sup>-1</sup>, respectively. The importance of operating conditions has been also shown in a study [39] with different desorption temperatures. In these experiments, the cooling power and COP are reported as 3.6 kW and 0.32, respectively, when the desorption temperature is 57 °C, and the cooling power and COP reach to 5.7 kW and 0.41, respectively when the desorption temperature is set at 80 °C. A cycle with both heat and mass recovery was also adopted in an experimental

study by Chen et al [40]. This compact silica gel/water adsorption chiller contains two adsorbent bed and one chilled water tank. The SCP and COP were reported as  $198 \text{ W kg}^{-1}$  and 0.49, respectively. In another experiment performed by Liu et al [41], applying heat and mass recovery cycle to an adsorption water chiller has increased the COP by 18.3% and the SCP by 13.7%. In this investigation, the system containing 26.4 kg of micro-pore silica gel with 0.7 mm average diameter demonstrates a COP of about 0.5 and SCP of  $341 \text{ W kg}^{-1}$ .

### **1.3.1.2 Thermo physical and adsorption properties**

Due to the growing application of silica gel adsorbent, some researchers put their effort on determining the thermo physical characteristics and adsorption properties of silica gel. The most important parameters that has been concerned so far are adsorptivity, thermal conductivity, heat capacity, diffusivity, granule size, porosity and permeability.

In a recent study performed by Wang et al. [42, 43], some different silica gel samples were prepared with various methods and tested in an adsorption refrigeration system. The parameters including surface area, silanol content, adsorption capacity, pore size distributions and deterioration were tested for all samples. The experimental results show that the adsorption capacity of the silica gel depends on many factors. However, pollution caused by solid particulates has significant impact on the adsorption capacity of silica gel granules. The adsorption characteristics of water onto two types of silica gel have been obtained in an experimental study [44]. Chua et al. has determined the thermo physical properties such as surface area, the density, pore size, pore volume, and total porosity of silica gel for type A and type RD. The adsorption capacity for both materials was calculated to be about 0.4 and  $0.45 \text{ kg}_w \text{ kg}_s^{-1}$ , respectively. In another study performed by Glaznev and Aristov [45], granule size impact on the performance of the cooling unit was investigated. The aim of this work was to compare the results for different sizes ranging from 0.2 to 1.8 mm. They have concluded that the radius size of the adsorbent has a dominant role on the dynamics of isobaric water adsorption and desorption. For large granules, the characteristic time was strongly dependent on the size and shape of the adsorbents. Effective thermal conductivity of

the adsorbent bed impacts the performance of the system significantly and therefore some researchers developed experimental set-ups to investigate the conductivity of the adsorbents individually. Usually, transient and steady state methods are used to determine the thermal characteristics of solid sorbents. In this regard, a comprehensive study has been conducted by Gurgel et al. [8]. They have developed a steady state and transient hot wire experimental set-up which its schematic view is shown in Figure 1.11. Thermal conductivity was determined using the stationary results and thermal diffusivity was calculated based on the results from transient conditions.

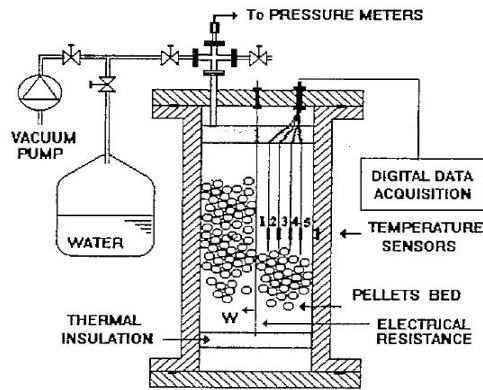


Figure 1.11: The schematic view of the thermal conductivity experimental set-up [8].

As shown in Figure 1.12, the thermal conductivity of silica gel increases with pressure at pressures less than 10 kPa. According to this work, another parameter influencing the thermal behavior of adsorbents is the water content of the materials which changes conductivity linearly. The experimental results show that the density, heat capacity, thermal conductivity and diffusivity of dry silica gel bed is  $746 \text{ kg m}^{-3}$ ,  $980 \text{ J kg}^{-1} \text{ K}^{-1}$ ,  $0.196 \text{ W m K}^{-1}$  and  $268 \times 10^{-9} \text{ m}^2 \text{ s}^{-1}$ , respectively.

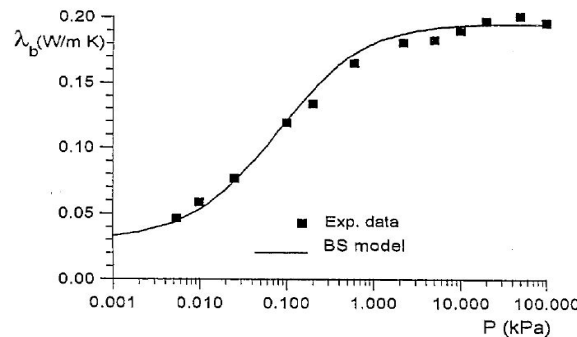


Figure 1.12: Thermal conductivity of a dry silica gel bed as a function of the air pressure (Pa) [8].



### **1.3.1.3 Modeling heat and mass transfer in porous media**

By developing the computers in recent years, researchers put more effort into simulating the adsorption phenomenon and heat and mass transfer in adsorbent bed using mathematical modeling. The advantages of this method over experimental studies are consuming less time and expenses together with producing more results which may not be possible to be achieved in experimental investigations. Governing equations related to heat and mass transfer inside the porous media has been studied widely in a review paper by Ge et al. [9]. In analyzing the gas flow through an adsorbent bed and process of adsorption, three types of heat and mass transfer forms occur from gas phase to solid phase which can be defined as resistances. Convective heat and mass transfer between gas and solid sorbent causes gas-side resistances from the gas to adsorbent surface. Also, diffusion and heat conduction occurs within the gas phase which is usually neglected since it is small in comparison to convective heat transfer. Solid-side resistances are from pore surface to its structure which is due to the heat conduction and mass diffusion within the adsorbent. Accordingly, established models in the literature are classified in two main categories: (1) gas-side resistance (GSR) model; (2) gas and solid-side resistance (GSSR) model [46].

In some cases in the literature, the SSR is not taken into account. Not considering the SSR is mainly due to the lack of complex diffusion relations inside the solid adsorbent. These models are developed in one-dimensional [47] and two-dimensional [46] form for more simplicity. Modeling the adsorption and desorption phenomenon without SSR leads to the omission of the heat conduction and mass diffusion terms within the porous material in mass and energy balance equations. Therefore, lower accuracy has been achieved in these models. However, recent theoretical models have been developed based on both gas-side and solid-side resistances. Differential element for a one-dimensional GSSR model is illustrated in Figure 1.13 [9].

Achieving high performances in adsorption chillers requires better transport of heat and mass inside the adsorbent bed. Therefore, many attempts have been made so far to simulate the heat and mass transfer characteristics of the adsorbent bed in adsorption cooling systems. However, the important point that should be taken into account is the relation between heat transfer resistances and mass transfer resistances. Some

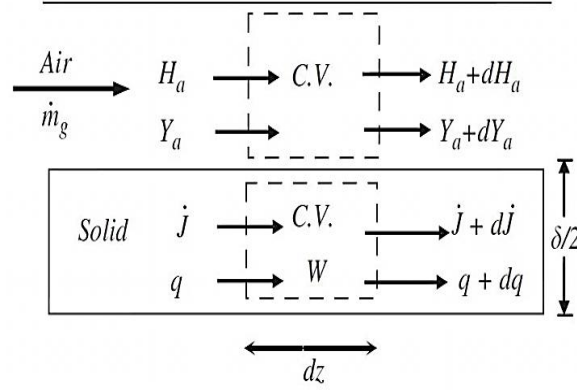


Figure 1.13: Differential element for a one-dimensional GSSR model [9].

investigations in the literature show that reducing heat transfer resistances inside a bed decreases the mass flow rate inside the bed. Therefore, heat and mass transfer phenomenon inside the bed should be analysed simultaneously to achieve the desired design of the bed [3]. In this regard, some coupled heat and mass transfer models have been developed and tested. In a study conducted by Solmus et al. [48], one and two-dimensional models were established and solved mathematically. The results show a good consistency with the experimental data. In another study by Caglar [11], transport inside the bed and adsorption phenomenon were simulated using COMSOL Multiphysics software and results were obtained for temperature distribution, pressure and water uptake of the adsorbents.

In another classification, the mathematical models are generally divided in two forms of local thermal equilibrium (LTE) and local thermal non-equilibrium (LTNE) models. The LTE models are based on the assumption that the temperature of the gas and solid phases are the same. Hence, one temperature is used which reduces the complexity of these models while sometimes yielding sufficient accuracy. LTE tends to be most accurate if the particles or pores are sufficiently small, the thermal properties are consistent and convective transport can be neglected. Also, there should be no significant heat generation in any of the phases. Otherwise, LTNE model should be considered for simulating the phenomenon. The validity and accuracy of the LTE model is investigated in a one-dimensional model developed by Solmus et al [48]. As shown in Figure 1.14, the temperature difference between the solid and gas phases is negligible except during the very early stages of the process which vanishes after a short period of time [3].

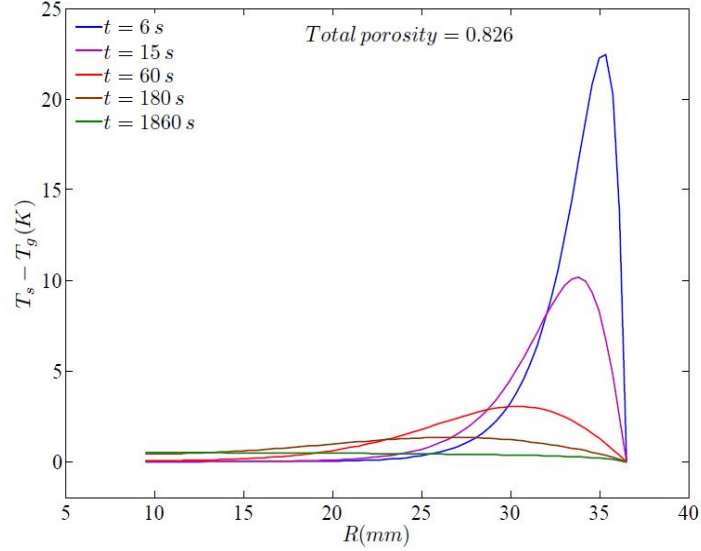


Figure 1.14: Temperature differences between the solid and gas phases in one-dimensional transient modeling [3].

### 1.3.2 Silica gel enhancements

Enhancements of adsorbents are investigated in two main aspects in previous studies. The first point is improving the rate of heat transfer without increasing mass transfer resistances. Heat and mass transfer have opposite relation with each other and reducing one causes the raise of the other. Increment of adsorption capacity of materials as well as transport enhancements is another important aspect. One solution to fulfil both objectives at the same time is to use more than one adsorbent in the adsorption bed. There are different methods to prepare the mixtures or composites that expose the desired characteristics. Adding metal pieces to the bed as well as mixing chemical and physical adsorbents are two modification methods that have been considered in the literature as a breakthrough.

#### 1.3.2.1 Additives

Simple mixture method is originally aimed to improve the thermal behavior of the adsorbents. Metal additives including copper, aluminum and stainless steel chips possess high thermal conductivity and diffusivity in comparison to conventional adsorbents and thus, raise the effective thermal conductivity of the mixture when added

to the adsorbents. However, presence of these additives increases the mass transfer resistances which consequently reduces the gas flow rate. To resolve this problem, investigations have been focused on determining the appropriate percentages of the additives in the mixture. For instance, thermal conductivity variations of zeolite adsorbent bed versus different percentages of copper chips were studied by Caglar [11]. In this work, a steady state thermal conductivity set-up was fabricated and copper chips in 16.6wt% and 25.1wt% proportions were added to the zeolite and mixed homogenously. As a result, the mixture with 25.1% copper chips showed the highest thermal conductivity among all samples. A more comprehensive study on this field has been conducted by Demir et al [10]. Also, different percentages of various metal additives are mixed with adsorbent silica gel and the thermal conductivity and diffusivity are calculated in a transient experimental set-up. The metal additives were supplied from a local raw material firm and sieved into two fractions as 1.0-2.8 mm and 2.8-4.75 mm as shown in Figure 1.15.



Figure 1.15: metal chips: a) copper; b) aluminum; c) stainless steel; d) brass [10].

The mixtures are tested in an experimental setup fabricated especially for this purpose. The results show a maximum diffusivity and conductivity enhancement of 157% and 242% was achieved, respectively for 15 wt% of Al additive. The minimum improvement of 33% belongs to 5 wt% of stainless steel additive. They have finally concluded that loading amount, thermal conductivity, diffusivity, shape and size are five important factors that affect the overall thermal behavior of the mixture.

### 1.3.2.2 Composites

As mentioned in the previous section, two main methods exist for improving the adsorption characteristics of silica gel adsorbents. Both approaches have been applied for silica gel enhancements and the results show better characteristics in terms of adsorptivity of the final product. Using these methods can also increase the permeability inside the adsorbent bed. The important factor increasing the water uptake of new composites is the presence of chemical adsorbents inside the porous structure which demonstrate higher affinity for water vapor. Calcium chloride ( $\text{CaCl}_2$ ), Lithium Bromide ( $\text{LiBr}$ ), Sodium chloride ( $\text{NaCl}$ ), Magnesium chloride ( $\text{MgCl}$ ) and Lithium chloride ( $\text{LiCl}$ ) are among the mostly utilized chemical adsorbents for this purpose. Chlorides and water can not be used as a solid sorption working pair, since  $\text{CaCl}_2$  liquefies after absorbing a certain amount of water. However, due to higher adsorption quantity of chemisorption materials, composite adsorbent with silica gel is mainly produced by addition of metal chlorides.

Composite adsorbents containing silica gel and chlorides are mainly developed by impregnation process, where the silica gel is immersed in a salt solution, and then dehydrated. Among metal chlorides, calcium chloride has attracted more attention due to its characteristics and availability. In the literature, two research groups have conducted some pioneer studies in the field of silica gel enhancements. Aristov and his colleagues [49, 50], have fabricated a number of composite adsorbents by confining metal chlorides to mesoporous silica gel in different proportions. They have named the new family of materials as Selective Water Sorbents, SWSs, which are produced by confining a salt in a porous host matrix. It was shown in their studies that water sorption characteristics of SWS can be controlled by varying the amount of confined salt and preparation procedure. The group of modified materials have been tested in an adsorption cycle and improvements have been reported in comparison to conventional silica gel. In another set of investigations in this field, Wang et al. [51, 52], have designed and fabricated a lab-scale adsorptive chiller and examined the adsorption characteristics of newly developed materials. Daou et al [52] have prepared and tested the adsorbent S40 (microporous silica gel impregnated in 40% concentrated solution of calcium chloride), and compared the COP and SCP values

with S0 (pure silica gel). The results show that the COP has been improved by 25% and water uptake capacity of S40 is more than twice of normal silica gel. Consolidated adsorbents are produced by compressing the composite powder prepared by impregnation. This kind of composite has the advantage of high thermal conductivity parallel to the compression. Wang et al. [53] demonstrated in another study that the combination of 4:1 between  $\text{CaCl}_2$  and activated carbon produce by consolidated method, possesses higher cooling density when compared to the granular composites. The cooling unit employing this kind of adsorbent had a maximum COP and SCP of 0.35 and  $493.2 \text{ Wkg}^{-1}$ , respectively which are 1.8 and 14 times higher than activated carbon/methanol pair. However, the number of fabrication processes necessary to achieve the final compound is counted as a disadvantage. Moreover, the mass transfer resistances are seriously increased which causes lower gas flow rate [7]. The preparation of composites is not limited to combination of just two adsorbents. In a recent investigation, Tso et al. [54], synthesized a new adsorbent with the combination of activated carbon, silica gel and calcium chloride. They have recorded a  $0.805 \text{ kg kg}^{-1}$  enhancement in equilibrium water uptake of the new product at atmospheric pressure. The final COP and SCP of the cooling unit is reported as 0.7 and  $378 \text{ Wkg}^{-1}$ , respectively.

The performance of commonly used conventional and advanced adsorbent and adsorbate working pairs are illustrated in Table 1.2, Figure 1.16 and Figure 1.17. As illustrated in the figure, metal hydrides and hydrogen working pair has the highest COP value which is 0.83. However, among the adsorption chillers with water refrigerant, silica gel and chloride composites demonstrate higher COP value.

Adsorption variations of different  $\text{CaCl}_2$  proportions in silica gel host matrix with relative humidity was investigated in a study by [52]. As can be inferred from the results, the increment in the equilibrium adsorption quantity decreases as the solution concentration is higher than 40%. The reason behind this result, is the fact that  $\text{CaCl}_2$  can easily liquefy during the adsorption process when the compound is prepared with a high concentration solution. Therefore, they have concluded that the ideal concentration to avoid such a problem and ensure high adsorption capacity would be the composite prepared in 40% concentration of salt in solution [7].

Importantly, choosing an ideal working pair in every aspect is not applicable for adsorption cooling applications and every system has an advantage over the others. However, based on the data analysed in this study, the combination of impregnated silica gel with calcium chloride and metal additives can produce the desired adsorption and desorption characteristics in terms of adsorptivity and heat and mass transfer inside the bed.

Table 1.2: The performance and working conditions for different working pairs [2].

	working pair	COP	SCP ( $\text{Wkg}^{-1}$ )	Evap.Temp	Driving Temp.
Physical adsorbent	Silica gel/water	0.61	208	5	82
	AC/methanol	0.78	2000	15	100
	AC/ethanol	0.8	16	3	90
	AC/ammonia	0.61	400	-5	80
	Zeolite/water	0.4	600	6.5	350
Chemical adsorbent	Metal chloride/ammonia	0.6	500	-10	52
	Metal hydrides/hydrogen	0.83	300	-50	85
	Metal oxides/water	0.29	78	100	200
Composite adsorbent	Silica gel and chlorides/water	0.8	800	7	70
	Silica gel and chlorides/methanol	0.33	240	-10	47
	Chlorides and porous media/ammonia	0.35	1200	-15	117.5
	Zeolite and aluminum/water	0.55	500	10	250

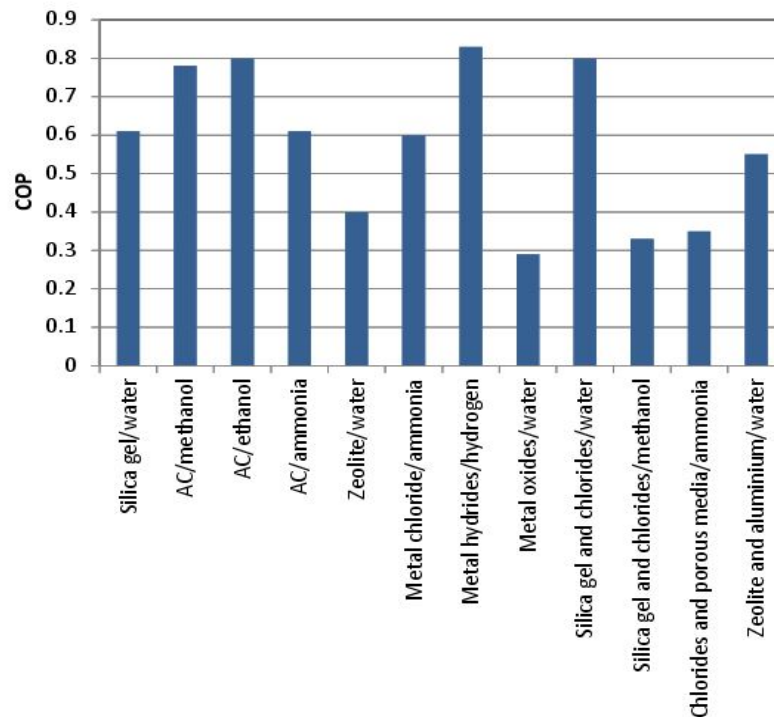


Figure 1.16: COP comparison for different working pairs [2].

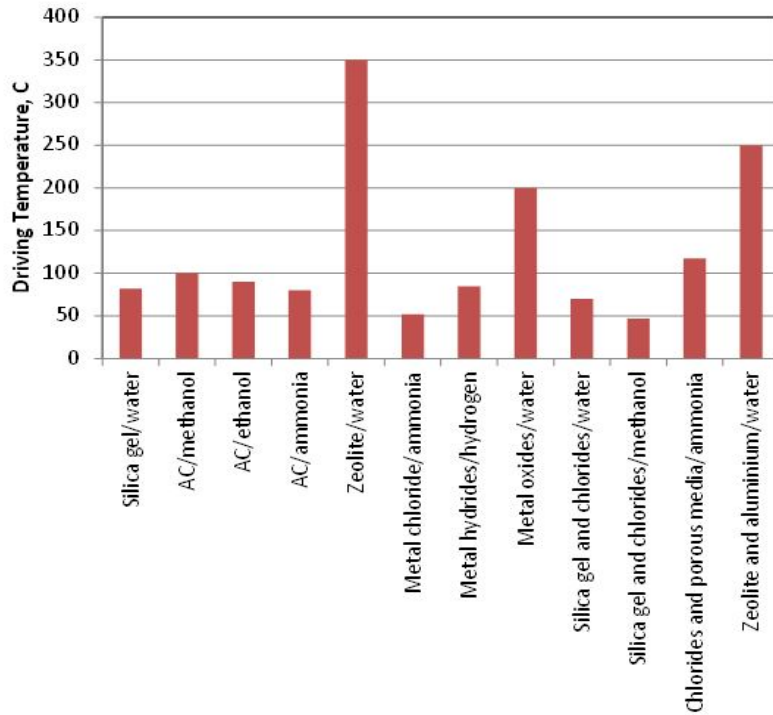


Figure 1.17: Driving temperature comparison for different working pairs [2].

#### 1.4 Objective and scope of the work

Generally, conventional adsorbents have low thermal conductivity and adsorptivity which causes lower COP and SCP of the system. According to the literature review section, some efforts have been made on improving the conventional adsorbents like silica gel in a variety of methods and satisfactory results have been obtained. However, there are still shortcomings which should be further fulfilled. Using metal pieces as additives inside the adsorbent bed is one solution that increases thermal conductivity of the bed. However, increasing the heat transfer coefficients causes higher mass transfer resistances and lower vapor flow rate. As a result, the adsorption process is affected by the increment of additives inside the bed. On the other hand, some methods like impregnation can be used to enhance the water uptake capacity of the adsorbents.

The **objective** of this work is to enhance thermal behavior and water uptake capacity of the adsorbent bed simultaneously. Hence, both metal additive and impregnation methods are utilized to increase the adsorption and desorption characteristics of the bed. For this purpose, the effects of metal additives and impregnation methods on



the performance of the cooling unit are investigated in theoretical and experimental works. In this study, silica gel is selected as the base adsorbent due to its features of regenerating in low temperatures and excellent compatibility with other adsorbents. A one-dimensional mathematical model is developed in COMSOL Multiphysics for studying the impact of important parameters on the adsorption and desorption characteristics in an adsorbent bed in real state conditions. Next, advanced materials are developed using methods described in chapter 3. In the third step, thermo physical properties of new materials are determined experimentally using steady state thermal conductivity test set-up and Brunauer- Emmett-Teller (BET) analysis in chapter 4. Finally, the material modification impacts on the performance of the cooling unit are investigated in an experimental set-up containing required components for adsorption cooling cycle. Attainable outputs of this study can be listed as a theoretical model which is capable of reporting the performance of an adsorbent bed in different working conditions and different adsorbents. Also, adsorbent materials with better characteristics for adsorption and desorption processes are fabricated and the influence of modifications are obtained in two different experimental facilities.



## **CHAPTER 2**

### **ONE-DIMENSIONAL NUMERICAL MODELING**

#### **2.1 Introduction**

Adsorbent bed is considered as the most important component in an adsorption cooling unit. Some complex phenomenon occur inside the bed simultaneously during the adsorption and desorption processes and many parameters take part on the performance of the bed. For this reason, in the first step, a mathematical model of the adsorbent bed was established in COMSOL Multiphysics to evaluate the factors affecting the heat and mass transfer mechanism and adsorption phenomenon.

The main objective in this chapter is to mathematically investigate the influence of design parameters and adsorbent properties on the temperature, pressure and water uptake of the adsorbent bed. To perform the investigation, governing equations of heat and mass transfer have been established based on the continuum theory using volume averaging method [26]. Then, the obtained equations have been solved in COMSOL Multiphysics Software. The base case analysis has been performed on silica gel/water working pair.

#### **2.2 Modeling procedure and fundamentals**

According to the configuration of the porous medium, modeling the transport of heat and mass between the voids can be performed in two forms of micro-scale and macro-scale. However, on the microscopic scale, the flow quantities like velocity and pressure irregularly change which makes the modeling process more complex. However,

by measuring the quantities over areas that cross many pores, such as space-averaged or macroscopic scale, quantities change in a regular manner with respect to space and time, and hence theoretical simulation of the real phenomenon can be applied accurately in a simplified form. This method has been applied widely for transport analysis in porous media. The details of the averaging method and deriving the conservation equations are explained in references [3, 26].

### 2.3 Model description

Figure 2.1 depicts the schematic view of the cylindrical adsorbent bed designed for performing the adsorption and desorption processes. The simulation data comprising the thermo physical properties of silica gel and bed geometry is given in Table 2.1. The bed consists of a cylinder with 70 mm in radius ( $r_o$ ) and a mass transfer tube with 5 mm in radius ( $r_i$ ). The space between the cylinder and mass transfer tube is filled with silica gel granules. During the adsorption, the water vapour enters the bed through the top of the mass transfer tube and flows from the outer surface of the mass transfer tube to the inner surface of the cylinder. In this study, a one-dimensional model of the bed is developed in COMSOL Multiphysics. Therefore, both ends of the bed cylinder are considered as insulated and heat and mass transfer is assumed to only occur in the radial direction.

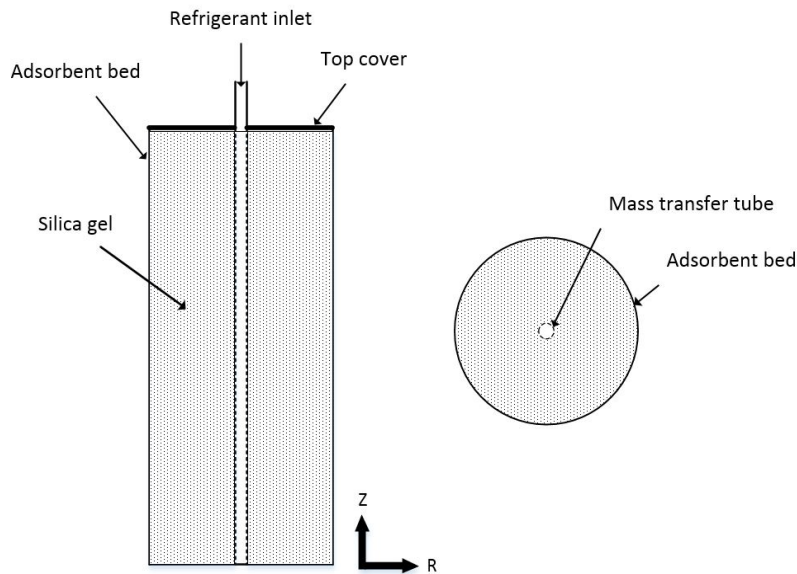


Figure 2.1: Schematic view of the cylindrical adsorbent bed.

## 2.4 Governing conservation equations

Three phases are considered during the adsorption process: 1. water vapor entering in gas phase; 2. adsorbed water on the surface of adsorbent in liquid phase ; and 3. adsorbent particles in solid phase. These phases are termed hereafter as the vapor phase, adsorbed phase and adsorbent, respectively. Therefore, there are “two-phase” fluid flow in a porous medium as shown in Figure 2.2.

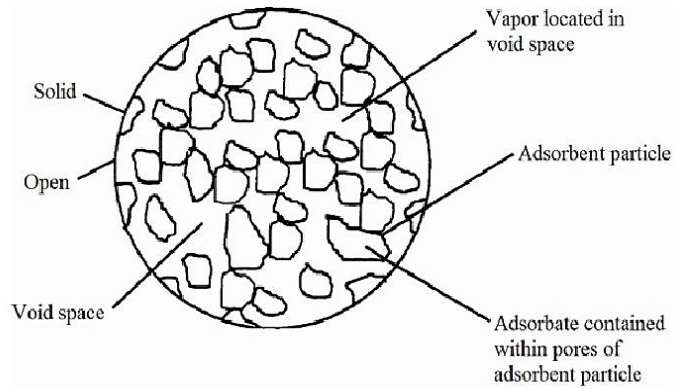


Figure 2.2: Two phase flow illustration in representative elementary volume [11].

In this model, the combination of adsorbed phase and adsorbent is considered as a single solid. Therefore, the model is two phase (vapor and solid) with single phase flow (vapor). Other assumptions of the current model are described as follows:

- The vapor phase is assumed to be an ideal gas;
- Radiative heat transfer, viscous dissipation and the work applied by pressure changes are neglected;
- The surface porosity is assumed to be same as total porosity;
- An average value is considered for physical properties (i.e. specific heat capacities, viscosity and thermal conductivities) which change with working conditions;
- The size of the adsorbent particles and bed porosity are spatially uniform;
- The thermal resistance due to wall thickness is neglected;

### 2.4.1 Mass conservation equation

Using the averaging method, macro scale mass conservation equation for the adsorbate gas can be written as:

$$\epsilon_t \frac{\partial(\rho_g)}{\partial t} + \frac{1}{r} \frac{\partial(r \rho_g \vec{\nu}_r)}{\partial r} + (1 - \epsilon_t) \rho_s \frac{\partial X}{\partial t} = 0 \quad (2.1)$$

The volume fraction of the gas phase,  $\epsilon_g$ , is assumed to be equal to the total porosity,  $\epsilon_t$ , and is calculated by,

$$\epsilon_t = \epsilon_b + (1 - \epsilon_b) \epsilon_p \quad (2.2)$$

Also, gas density,  $\rho_g$ , is a function of pressure and temperature and is calculated using the following equation:

$$\rho_g = \frac{P}{R_g T} \quad (2.3)$$

### 2.4.2 Momentum conservation equation

Darcy's equation is used for calculating the velocity of adsorbate gas in the adsorbent bed. Darcy's equation is given in the following equation:

$$\vec{\nu}_r = - \frac{\lambda}{\mu_g} \frac{\partial P}{\partial r} \quad (2.4)$$

In the above equation,  $\lambda$  is the real permeability which is calculated using the Blake-Kozeny equation,

$$\lambda = \frac{d_p^2 \epsilon_b^3}{150(1 - \epsilon_b)^2} \quad (2.5)$$

### 2.4.3 Energy conservation equation

As mentioned in the literature review section, the temperature gradients between the vapor and solid phases dies out after a short time from the beginning of the adsorption process. Therefore, local thermal equilibrium model can be assumed during energy transport inside the adsorbent bed and only one energy conservation equation is sufficient for accurate simulation. Due to this reason, the governing energy equation is derived for the gas and solid phases using the local averaging solution. Final form of the energy equation is given in the following equation:

$$C_{pg}\rho_g \left[ \epsilon_t \frac{\partial T}{\partial t} + \vec{\nu}_r \frac{\partial T}{\partial r} \right] = \frac{1}{r} \frac{\partial}{\partial r} \left( r k_{eq} \frac{\partial T}{\partial r} \right) + \rho_s (1 - \epsilon_t) \frac{\partial X}{\partial t} Q_{ad} - \rho_s (1 - \epsilon_t) [C_{ps} + X C_{pl}] \frac{\partial T}{\partial t} \quad (2.6)$$

In the above equation,  $k_{eq}$  is the total thermal conductivity for the solid and gas phases which can be defined as follow:

$$k_{eq} = k_{se} + k_{ge} + k_{le} \quad (2.7)$$

In the above equation,  $k_{se}$ ,  $k_{ge}$  and  $k_{le}$  are solid, vapor and adsorbed liquid phase thermal conductivity, respectively. These parameters are calculated using the equations below:

$$k_{se} = (1 - \epsilon_t) k_s \quad \text{and} \quad k_{ge} = \epsilon_t k_g \quad \text{and} \quad k_{le} = (1 - \epsilon_t) X k_l \quad (2.8)$$

The heat of adsorption,  $Q_{ad}$  for the silica gel/water working pair is considered to be equal to 3300 kJ/kg [25].

### 2.4.4 Adsorption auxiliary equation

In this section, in order to complete the set of required equations for modeling, some auxiliary correlations have been provided. During the process of adsorption, vapor

flow occurs from the outside of an adsorbent particle to the surface of the material and an adsorbed state inside the particle. For this reason, vapor mass flow rate and internal mass transfer resistances within the adsorbent particles should be considered. The Linear Driving Force (LDF) model is used to simulate the process of adsorption inside the bed. The LDF equation is defined as follow:

$$\frac{\partial X}{\partial t} = k_m(X_\infty - X) \quad (2.9)$$

In the above equation,  $k_m$  is the internal mass transfer coefficient which is calculated by

$$k_m = 60D_e/d_p^2 \quad (2.10)$$

$D_e$  is the equivalent diffusivity of the adsorbent which is defined as [3]

$$D_e = D_0 \exp(-E_a/R_g T) \quad (2.11)$$

The final adsorption equation is expressed as

$$\frac{\partial X}{\partial t} = \frac{60D_0 \exp(-E_a/R_g T)}{d_p^2} (X_\infty - X) \quad (2.12)$$

the modified Dubinin-Astakhov (D-A) equation is used to calculate the equilibrium adsorption capacity ( $X_\infty$ ) of the adsorbents.

$$X_\infty = X_{ad_0} \exp[-A(T/T_{sat} - 1)^n] \quad (2.13)$$

In the above equation,  $A$ ,  $n$  and  $X_{ad_0}$  are the D-A constants. Saturation temperature is calculated using the following equation:

$$T_{sat} = 39.7240 + \frac{1730.63}{(8.07131 - \log |P| \times 7.500638 \times 10^{-3})} \quad (2.14)$$



### 2.4.5 Initial and boundary conditions

The initial and boundary conditions of the model are specified in this section. The variables are temperature, pressure and amount-adsorbed which have the following values in the beginning of the simulation.

$$T(0, r) = T_i \quad \text{and} \quad P(0, r) = P_i \quad \text{and} \quad X(0, r) = X_i \quad (2.15)$$

The following conditions are assumed at the inner surface of the bed. The adsorbed gas pressure is assumed to be equal to the evaporator pressure at the beginning of adsorption process and equal to condenser pressure as the desorption process starts. Also, the temperature gradient at this point is zero due to adiabatic surface condition. The domain modeled in COMSOL and defined boundary conditions are shown in Figure 2.3.

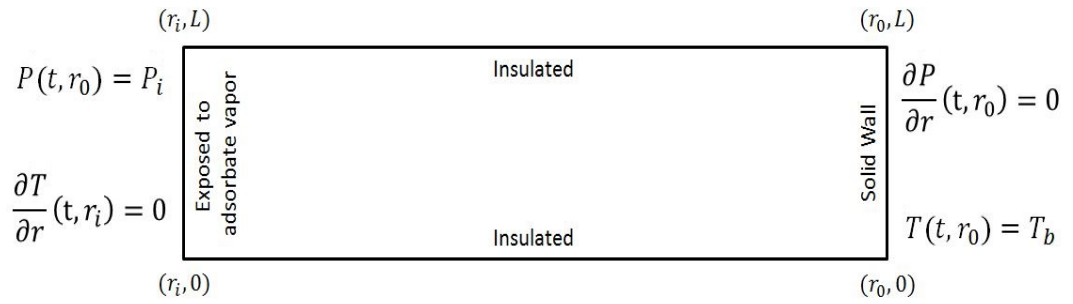


Figure 2.3: Modeling domain with boundary conditions.

$$P(t, r_i) = P_i \quad \text{and} \quad \frac{\partial T}{\partial r}(t, r_i) = 0 \quad (2.16)$$

At the wall surface of adsorbent bed, pressure gradient is zero. Therefore, we have following conditions at this boundary:

$$\frac{\partial P}{\partial r}(t, r_o) = 0 \quad \text{and} \quad T(t, r_o) = T_b \quad (2.17)$$

The thermo physical properties of silica gel/water working pair and working conditions used in this study are presented in Table 2.1.

Table 2.1: Model parameters [3].

Parameter	Value	Unit
$A$	5.6	D-A equation constant
$n$	1.6	D-A equation exponent
$D_o$	2.54E-04	$\text{m}^2\text{s}^{-1}$
$d_p$	3.20E-03	m
$E_a$	4.20E+04	$\text{Jmol}^{-1}$
$R$	8314	$\text{Jmol}^{-1}\text{K}^{-1}$
$\rho_s$	670	$\text{kg m}^3$
$c_{ps}$	880	$\text{Jkg}^{-1}\text{K}^{-1}$
$c_{pg}$	1840	$\text{Jkg}^{-1}\text{K}^{-1}$
$k_s$	0.198	$\text{Wm}^{-1}\text{K}^{-1}$
$k_g$	0.0196	$\text{Wm}^{-1}\text{K}^{-1}$
$k_l$	0.65	$\text{Wm}^{-1}\text{K}^{-1}$
$\mu_g$	1.00E-05	$\text{kgm}^{-1}\text{s}^{-1}$
$\epsilon_b$	0.37	
$\epsilon_p$	0.42	
$Q_{ad}$	3300	$\text{kJ kg}^{-1}$
$X_{ado}$	0.346	
$c_{pl}$	4180	$\text{Jkg}^{-1}\text{K}^{-1}$
$R_g$	461.5	$\text{Jkg}^{-1}\text{K}^{-1}$
$r_o$	70	mm
$r_i$	5	mm
$P_{ev}$	1.228	kPa
$P_{con}$	4.247	kPa
$T_i$	363	K
$T_b$	303	K

## 2.5 Solution to model

The solution methods generally used in the literature compromise finite difference, finite volume and finite element methods. Among these methods, finite difference has the advantage of simplicity. However, finite element and finite volume methods are capable of producing more accurate outputs. Therefore, to obtain more accuracy, the finite element method is chosen. On the other hand, due to the complexity and nonlinearity of the adsorption and desorption model, COMSOL Multiphysics is applied for solving the set of coupled heat and mass transfer equations. COMSOL Multiphysics is a new type of software package which is used for solving multidisciplinary phenomenon simultaneously. Different engineering modules exist in the

library of this software which are specifically designed for solving engineering problems. In addition to availability of modules for a specific phenomenon, a PDE solver module exists for solving any auxiliary equation. Using these features, the modules used in this study are "Heat Transfer" for energy equation, "Darcy's law" for mass conservation and momentum equations and a "Coefficient form PDE" for LDF model equation. This software is also capable of solving both transient and steady state systems in one, two or three dimensions. The graphical and user friendly environment of the modeling process, facilitates the simulation of complex systems. After inserting the equations and defining the initial and boundary conditions in the specified spaces in each module, the next step is to complete the meshing process. The user is permitted to manually insert the range and size of meshes or select one of the predefined meshing options. The post processing part starts after calculating the defined variables in every nodes. In this study, the temperature, pressure and water uptake capacity distributions were plotted as a result to investigate the important parameters affecting the heat and mass transfer and adsorption phenomenon inside the bed.

## 2.6 Results and discussions

The model has been solved for adsorption and desorption process inside the bed using the specified data in Table 2.1 for silica gel/water working pair. Figure 2.4, shows the geometry of the model developed in COMSOL Multiphysics. The points 1 to 6 are at 65 mm, 55 mm, 45 mm, 35 mm, 25 mm and 15 mm distance from the cylinder wall, respectively.

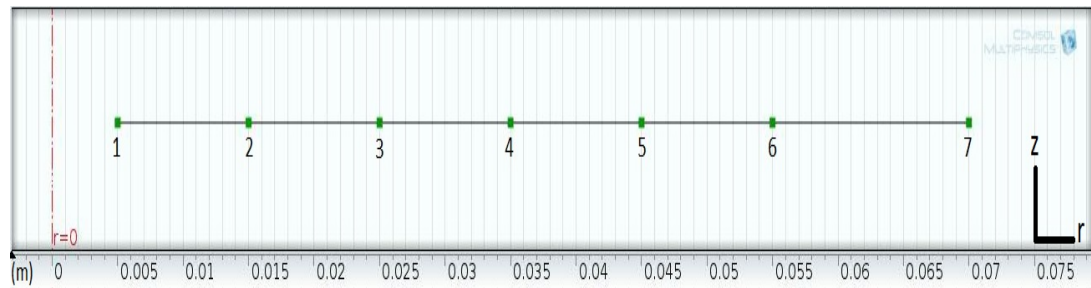


Figure 2.4: Schematic view of the one-dimensional symmetrical model in COMSOL Multiphysics. The points 1 to 6 are at 65 mm, 55 mm, 45 mm, 35 mm, 25 mm and 15 mm distance from the cylinder wall, respectively.

### 2.6.1 Base case study

The thermal behavior of adsorbent bed and temperature distribution is illustrated in Figure 2.5. According to initial and boundary conditions, the temperature at wall (point 7) is set at 30 °C and the bed is initially at 90 °C. The bed is cooled from 90 °C to 30 °C gradually and adsorption process occurs at the same time. As can be seen in Figure 2.5, at the beginning of adsorption process, there is a slight increment in temperature which is due to the heat of adsorption. The water vapor is adsorbed until the bed temperature and water uptake reach to steady state conditions. Figure 2.6 shows the amount of water vapor adsorbed inside the bed. The process of adsorption continues until no more adsorption takes place and the value for water uptake capacity is fixed. During adsorption process the boundary pressure at point 1 is equal to evaporator pressure.

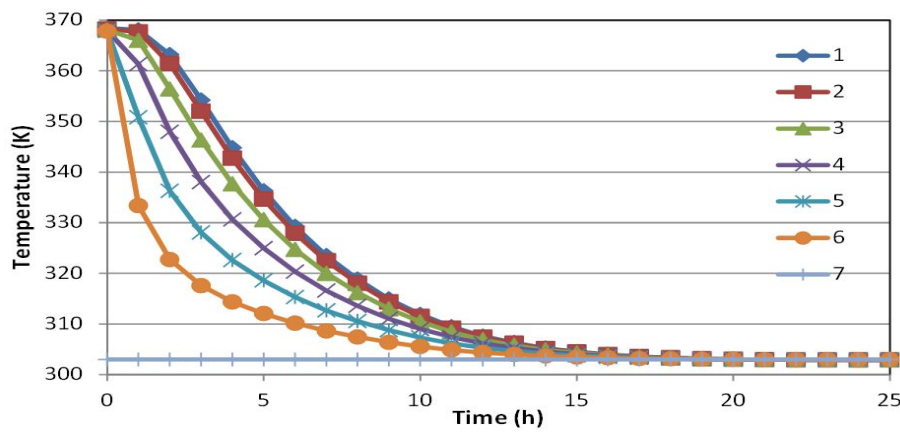


Figure 2.5: Temperature distribution during adsorption process inside the bed.

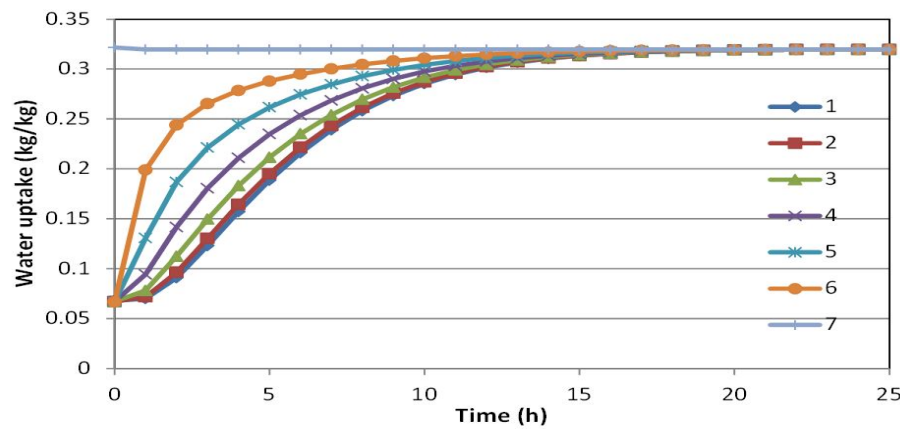


Figure 2.6: Water uptake amount during adsorption process inside the bed.

During the desorption process, the wall temperature is set at  $90^{\circ}\text{C}$  and the bed temperature is initially at  $30^{\circ}\text{C}$ . The temperature distribution inside the bed is shown in Figure 2.7 in radial direction for silica gel. For desorption, the bed is initially at condenser pressure and the inner surface of the bed is also at condenser pressure.

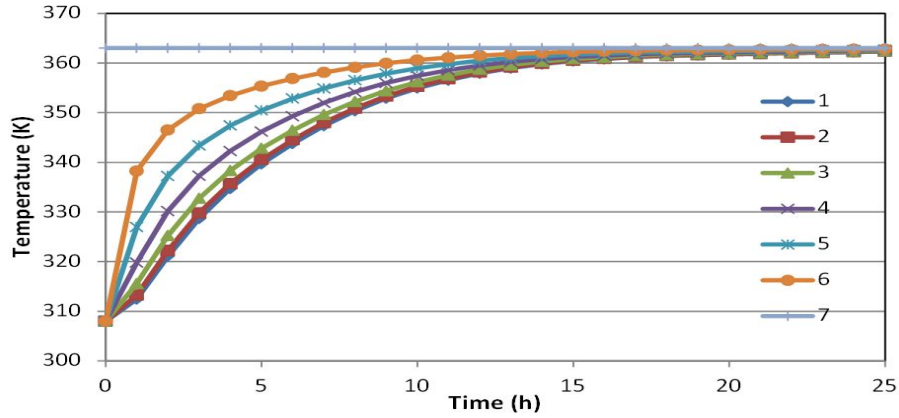


Figure 2.7: Temperature distribution during desorption process inside the bed.

### 2.6.2 Effect of thermal conductivity of solid phase on the adsorption and desorption processes

After solving the equations in COMSOL, the design parameters affecting the performance of the adsorbent bed is investigated. According to the objective of this study, the adsorption characteristics of the bed is analyzed for different thermal conductivity values. For this purpose, thermal conductivity is fixed at 1, 0.75, 0.5, 0.3, 0.198 and  $0.1 \text{ W m}^{-1} \text{ K}^{-1}$  and results obtained for point 4 in the middle of the bed. As shown in Figure 2.8, the adsorption process ends more quickly as the thermal conductivity of the bed rises. The bed reaches to steady state condition faster and therefore, the cycle time reduces significantly. The same behavior is also demonstrated in Figure 2.9 for the amount of adsorbed water. Water is adsorbed more quickly while heat transfer rate is higher and the bed gets cool in shorter time.

The temperature distribution during the desorption process is illustrated in Figure 2.10 at point 4 for different thermal conductivities. As can be inferred from this figure, the bed temperature increases more quickly at higher thermal conductivity values resulting in shorter cycle time.

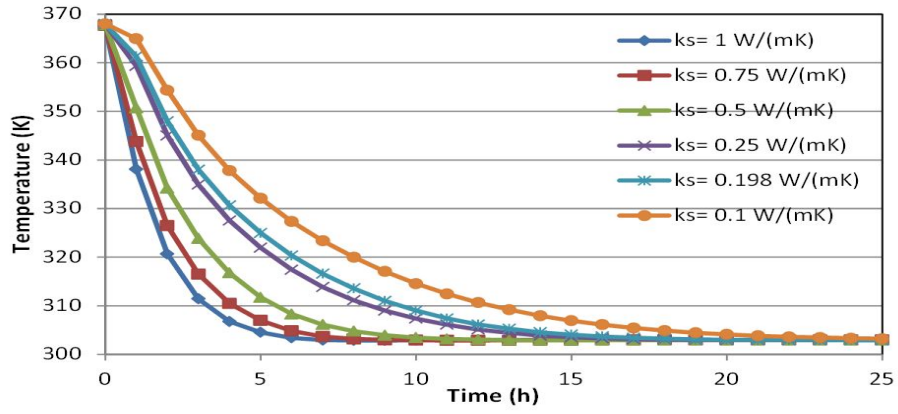


Figure 2.8: Temperature distribution during adsorption process for different thermal conductivity values.

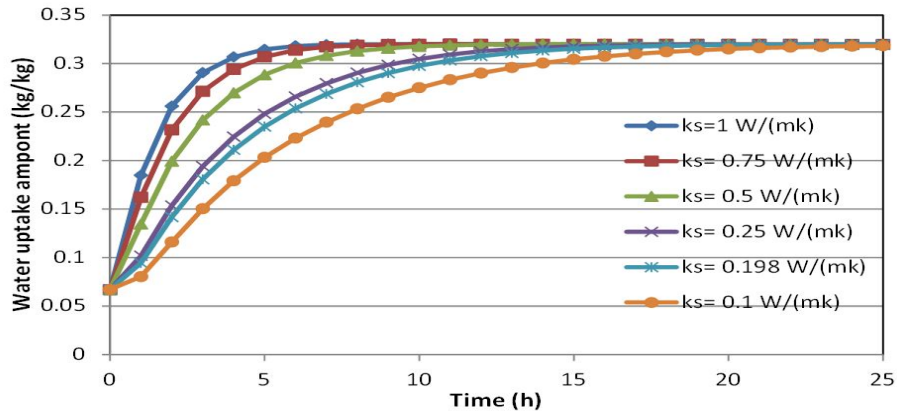


Figure 2.9: Water uptake amount during adsorption process for different thermal conductivity values.

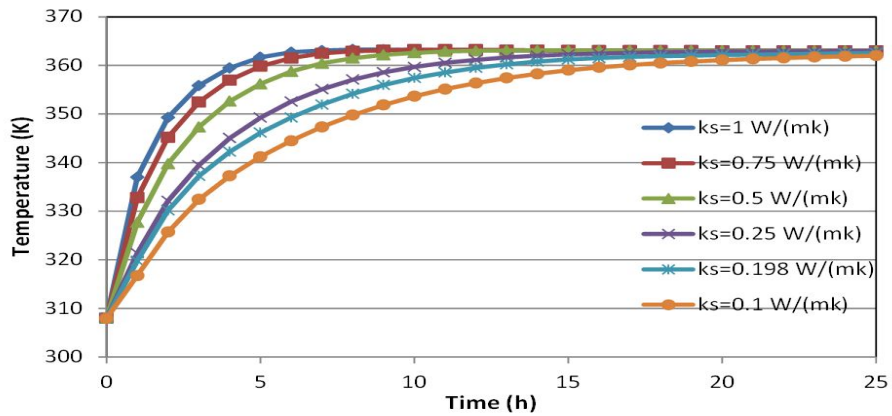


Figure 2.10: Temperature distribution during desorption process for different thermal conductivity values.

## **CHAPTER 3**

### **MATERIAL PREPARATION AND FABRICATION**

#### **3.1 Introduction**

Part of the objective of this thesis is to enhance the adsorption and desorption characteristics of silica gel to make silica gel more suitable for use in adsorption and desiccant cooling systems. The heat and mass transfer inside the bed and water uptake capacity of adsorbents are two dominant parameters that significantly influence the performance of the system. Heat transfer rate can be increased by developing adsorbents with higher thermal conductivity and diffusivity. Also, water uptake capacity of adsorbents can be enhanced when mixed with other adsorbents. In this chapter, the methods used for fabricating and developing silica gel are illustrated and the modification process is described in detail. The characteristics of developed materials have been tested in a set of experiments explained in the following chapters.

#### **3.2 Silica gel preparation**

The conventional silica gel granules was supplied from Damlakimya Co. The thermo physical properties of amorphous form of silica gel is given in Table 3.1 [6]. Before starting the modification processes, the silica gel granules must be prepared in advance. For this purpose, silica gel was dehydrated inside an oven at 95 °C and weighed every 30 minutes during the drying process. Once there is less than 1gr difference between two measurements, the materials are considered ready to be used. The supplied silica gel granules are shown in Figure 3.1.

Table 3.1: The thermo physical properties of silica gel [3].

properties	Value	Unit
Chemical formula	SiO <sub>2</sub> . n(H <sub>2</sub> O)	-
Average pore diameter	2-14	nm
Specific Surface area	340-800	$m^2g^{-1}$
Particle density	0.62-1.09	$gcm^{-3}$
Bulk Density	720	$gL^{-1}$
Thermal conductivity	0.198	$Wm^{-1}K^{-1}$
Heat capacity	921	$Jkg^{-1}K^{-1}$
porosity	0.635	
Heat of adsorption	2800	$kJkg^{-1}$
Adsorption quantity	0.34	$kg_wkg_s^{-1}$
Granule diameter	2-3	mm



Figure 3.1: Picture of the supplied silica gel granules.

### 3.3 Enhancements in desorption characteristics

Thermal conductivity and diffusivity of the commonly used adsorbents are still low which yields to higher energy consumption and increased cycle time. One way to enhance heat transfer characteristics is by adding metal pieces to the adsorbent bed. Metal additives like copper, aluminum and stainless steel possess higher thermal characteristics in comparison to silica gel and thus decrease the heat transfer limitations inside the bed when mixed with the adsorbent. In addition to thermal properties, the size and shapes of the additives also affect the behavior of final product. In this study, the aluminum chips were supplied from a raw material firm in OSTIM and cut into pieces at METU laboratory. For better results in mass transfer, metal pieces are prepared in small shapes which have characteristic lengths between 2-4 mm. Then, the pieces are washed with alcohol and sieved into the desired sizes as shown in Figure 3.2. In the next step, different weight and volume percentages of metal additives were



mixed with the silica gel uniformly. The properties of metal additives that are used in this study are presented in Table 3.2.

Table 3.2: Thermo physical properties of aluminum metal chips.

Material	Aluminum
Thermal Conductivity( $\text{Wm}^{-1}\text{K}^{-1}$ )	237
Density ( $\text{kgm}^{-3}$ )	2702
Specific Heat ( $\text{Jkg}^{-1}\text{K}^{-1}$ )	903
Thermal Capacitance ( $\text{Jm}^{-3}\text{K}$ )	$2.4 \times 10^6$
Thermal Diffusivity ( $\text{m}^2\text{s}^{-1}$ )	$9.71 \times 10^{-5}$



Figure 3.2: Picture of the prepared aluminum metal additive.

### 3.4 Enhancements in adsorption characteristics

According to the literature, two methods are implemented to increase water uptake capacity of conventional adsorbents: impregnation and consolidation. The impregnation method produces large porosity inside the media which causes mass transfer enhancement. Consolidated adsorbents show higher thermal conductivity but increases the mass transfer resistances due to more compact structure. Also, more operation steps are necessary to fabricate this type of composite. Therefore, in this study, impregnated method is applied to enhance the adsorptivity of conventional silica gel. In the literature, confining calcium chloride in a silica gel structure is shown to demonstrate higher adsorption capacity in comparison to other chemical adsorbents. Therefore,  $\text{CaCl}_2$  was chosen as supplementary adsorbent in the process of impregnation. Calcium chloride is supplied from Birpa Co. which is shown in Figure 3.3.

The impregnation process of confining the calcium chloride adsorbent into the pore



Figure 3.3: Picture of the supplied calcium chloride.

structure of silica gel consists of four steps. First, the supplied calcium chloride in solid form was dissolved in distilled water. The amount of calcium chloride and water was prescribed according to the specified calcium chloride proportion in the solution. Then, the solution was kept at 25 °C (ambient temperature) for two hours. In order to speed the dissolution process and preventing the crystallisation, the solution was stirred every 5-10 minutes. In the next step, silica gel granules were immersed in the prepared solution and kept in ambient temperature for twelve hours to allow the salt solution to penetrate and fill all the pore volumes. In the next step, the composition of silica gel and calcium chloride was sieved and kept in ambient temperature for a short time to let out the poorly concentrated solution. The rest of the process is same as the step for silica gel preparation. In this study, three different amounts of 20wt%, 40wt% and 60wt% of calcium chloride in relation to the total weight of solution were prepared. The samples were dehydrated in an oven at 95 °C and weighed every 30 minutes during the drying process. Once there is less than 1gr difference between two measurements, the developed materials are considered ready to be tested in experimental investigations. The prepared samples are called S20, S40 and S60 based on the weight percentages of calcium chloride inside the solution. The picture of the final impregnated silica gel is shown in Figure 3.4.

The properties of fabricated materials and enhancements were determined in experimental investigations. A setup were developed to obtain the thermal conductivity of the materials and mixtures. Moreover, the physical properties of impregnated materials were determined in Central Laboratory at METU. Finally, the influence of metal additives and impregnation process on water uptake capability and thermal behavior

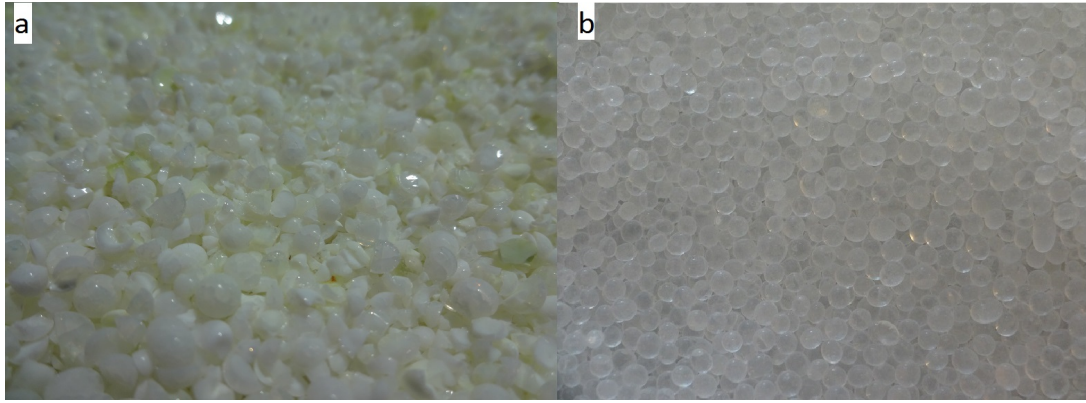


Figure 3.4: The picture of (a) final impregnated silica gel; (b) unmodified silica gel.

of the adsorbent bed were investigated experimentally in an adsorption cooling set-up constructed in Heat Transfer Laboratory at Mechanical Engineering Department, METU. An overview of different experimental investigations and tested materials are described In Table 3.3.

Table 3.3: An overview of different experimental investigations and tested materials.

Investigation	Analysis	place	Samples
Thermal Conductivity	Steady state conductivity	Heat Transfer Laboratory, METU	Silica gel dry Silica gel with 2 % Aluminum Silica gel with 5 % Aluminum Silica gel with 10 % Aluminum S20 S40 S60
Heat Capacity	TAL (DSC)	Central Lab., METU	Silica gel S20 S40 S60
Pore diameter and surface area	BET analysis	Central Lab., METU	Silica gel S20 S40 S60
Adsorption capacity	LTE adsorption	Heat Transfer Laboratory, METU	Silica gel S40
Silica gel with 10 % Aluminum			

## **CHAPTER 4**

### **EXPERIMENTAL INVESTIGATIONS ON THERMO PHYSICAL PROPERTIES OF ADSORBENTS**

#### **4.1 Introduction**

As indicated in chapter two, the thermo physical properties of adsorbents have significant influence on the thermal and transport behavior of the bed and consequently the performance of the cooling unit. In this study, new composites and mixtures have been prepared. Hence, determining the characteristics of these new products is vital. The thermal conductivity, specific heat capacity and thermal diffusivity of adsorbents are considered as thermal properties and density, porosity and permeability are physical properties of porous structure substances. This chapter covers the experimental works for calculating effective thermal conductivity, specific heat capacity, pore size and surface area of the developed adsorbents.

#### **4.2 Thermal conductivity investigation**

There are generally two methods to measure the thermal conductivity of porous materials: steady state and transient methods. Also, different techniques are used for measuring the thermal conductivity in both steady state and transient methods: 1) the guarded hot-plate; 2) longitudinal bar; and 3) flash thermal diffusivity method [55]. The first two are steady state methods and the third one is a transient method. In this study, the steady state hot-plate method was chosen due to the simplicity and available facility in the lab. The application of transient method is more complex and requires

the measurement of temperature change with respect to time. However, when the steady state method is applied the measurements take longer.

#### 4.2.1 Thermal conductivity experimental set-up

The Hot-Plate steady state thermal conductivity measurement method is used and the set-up shown in Figure 4.1 has been developed at METU, heat transfer laboratory to determine the thermal conductivity of materials. The test facility shown in Figure 4.2 contains three copper plates which are placed at the same distance from each other. The plate in the middle is surrounded by resistance wire which is connected to the power supply. The side, top and bottom walls are well insulated by fibreglass materials. Thermocouples are installed on the inner surface of the middle and front plates in five different positions. The thermocouples are connected to the data logger device. The mean value reported from the data logger is considered as the temperature of the plates. The specifications of the set-up is given in Table 4.1.

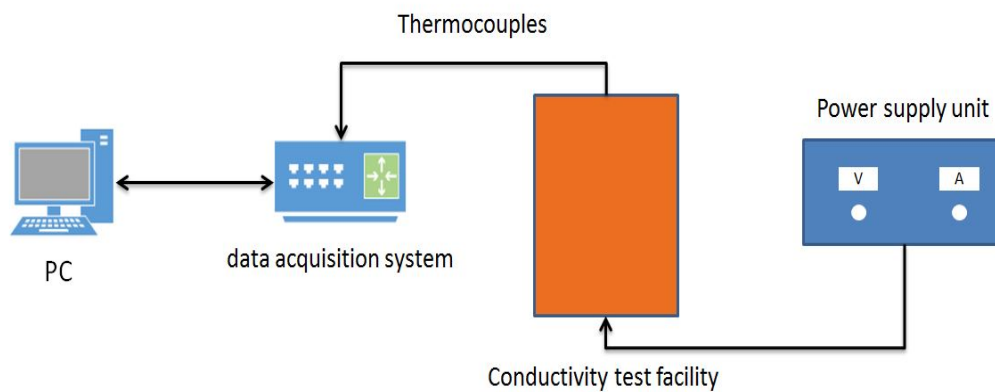


Figure 4.1: Thermal conductivity test set-up.



Figure 4.2: Picture of the conductivity test facility.

Table 4.1: Specifications of the conductivity set-up.

Parameter	value	unit
Length of the plates	20	cm
Width of the plates	15	cm
Inner distance between the plates	3	cm
The width of the installation	2	cm
Thermal conductivity of the fibreglass	0.04	$\text{W m}^{-1} \text{K}^{-1}$

#### 4.2.2 Test procedure

During the experiments, the mixtures and composites are prepared as indicated in previous chapter and then are homogeneously put inside the set-up. Next, the voltage and current of the power supply is fixed on the specified values and the test begins. After 4-7 hours, the temperature of the system rises and finally reaches to a steady state condition with the surroundings. The temperatures at the steady state condition are recorded and used for thermal conductivity calculations.

#### 4.2.3 Result and discussions

The tests were performed for the samples indicated in Table 3.3. The obtained temperatures are used in the steady state heat flow equation to calculate the effective thermal conductivity values.

$$Q = -kA \frac{\Delta T}{\Delta x} \quad (4.1)$$

Where  $\Delta T/\Delta x$  is the temperature gradient at the steady state condition and  $Q$  is the amount of heat in watts flowing through a cross-sectional area  $A$ . The heat power is calculated by multiplying the values for voltage and current:

$$Q = P = VI \quad (4.2)$$

Table 4.2 shows the experimental data and obtained results for the conducted thermal conductivity tests. The values for thermal conductivity of pure silica gel are close to the range of thermal conductivities reported in the literature [10, 8].

Table 4.2: Experimental data and obtained results for the thermal conductivity measurements.

Samples	volume fraction (%)	weight fraction (%)	Tresist. (°C)	Tad. (°C)	Effective thermal conductivity (W m <sup>-1</sup> K <sup>-1</sup> )	mean value for thermal conductivity (W m <sup>-1</sup> K <sup>-1</sup> )	Improvement (%)
silica gel	-	-	51.85	39.25	0.1879	0.1935	
			72.5	47.3	0.1909		
			91.1	53.22	0.1954		
			106.86	59.66	0.1997		
Al-Si	2	7.11	46.1	35.3	0.2232	0.2345	21.2
			67.62	46.67	0.2305		
			82.8	51.67	0.2401		
			97.88	58.75	0.2442		
Al-Si	5	16.4	45.5	36.22	0.2453	0.2625	29.4
			63.97	44.41	0.251		
			83.35	56.01	0.2757		
			97.14	62.47	0.2778		
Al-Si	10	29.4	44.5	36.32	0.2812	0.2928	37.8
			60.97	43.45	0.2845		
			81.5	56.1	0.2985		
			96.85	65.51	0.307		
S20			50.85	38.34	0.1914	0.1976	2.1
			70.49	47.56	0.1958		
			90.07	55.5	0.1974		
			104.29	61.49	0.2058		
S40			47.21	37.22	0.1998	0.2058	6.4
			70.04	47.68	0.2014		
			88.98	56.29	0.2097		
			103.54	62.03	0.2124		
S60			48.56	38.95	0.2045	0.2161	11.7
			67.85	46.48	0.2131		
			88.56	57.6	0.2217		
			101.96	62.55	0.225		



The obtained results also demonstrate that among the mixtures considered using aluminum as metal additive increases the conductivity of the mixture the most. The mixtures with 2, 5 and 10 volume percentages of aluminum chips increase the thermal conductivity by 21.2%, 29.4% and 37.8%, respectively. The variations of results for thermal conductivity of the samples with temperature are shown in Figure 4.3. According to this figure, there is a gradual increment in the conductivity of samples as the power and temperature increase. The reason behind this behavior is mainly due to the dependence of conductivity on temperature. Also, growth in heat losses at higher temperatures increases the measured thermal conductivities (where measured and true thermal conductivities are different due to experimental errors). On the other hand, the determined thermal conductivity values for impregnated adsorbents show a slight improvement in comparison to pure silica gel.

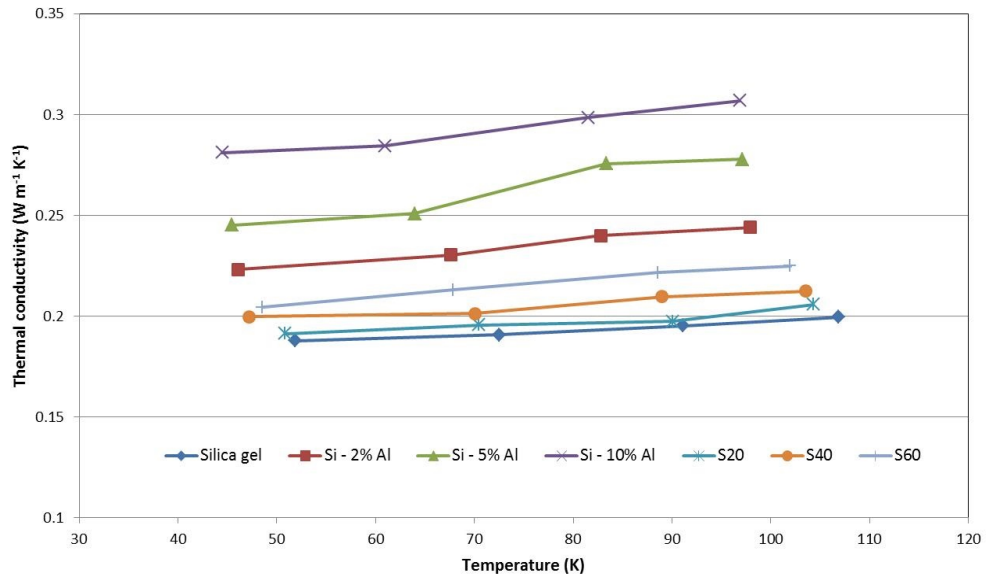


Figure 4.3: The variations of results for thermal conductivity of the samples with temperature.

#### 4.2.4 Effective thermal conductivity model

Several models have been developed to predict the effective thermal conductivity of solid mixtures with two phases. In a study performed by Wang et al. [56], five fundamental methods are described which are applicable based on the structure of the mixtures. For a mixture with one continuous and one dispersed phases, Maxwell-

Eucken (ME) method is used expressed as:

$$k_{eq} = \frac{k_2\epsilon_2 + k_1\epsilon_1 \frac{3k_2}{2k_2+k_1}}{\epsilon_2 + \epsilon_1 \frac{3k_2}{2k_2+k_1}} \quad (4.3)$$

In the above equation,  $k_1$ ,  $k_2$  and  $\epsilon_1$ ,  $\epsilon_2$  are the thermal conductivity and volume fraction of metal additive and pure silica gel, respectively. The results for experimental and theoretical tests are shown in Table 4.3.

Table 4.3: The results for experimental and theoretical investigations on mixture thermal conductivity.

Samples	Mean value for thermal conductivity (W m <sup>-1</sup> K <sup>-1</sup> )	Thermal conductivity obtained from mixture model (W m <sup>-1</sup> K <sup>-1</sup> )	Error %
silica gel	0.1935		
Si - 2% Al	0.2345	0.21	11.7
Si - 5% Al	0.2625	0.229	14.6
Si - 10% Al	0.2928	0.264	10.9

Figure 4.4 illustrates the results for silica gel and aluminum mixtures in different proportions. As shown in this figure the experimental data are in good consistency with results from model.

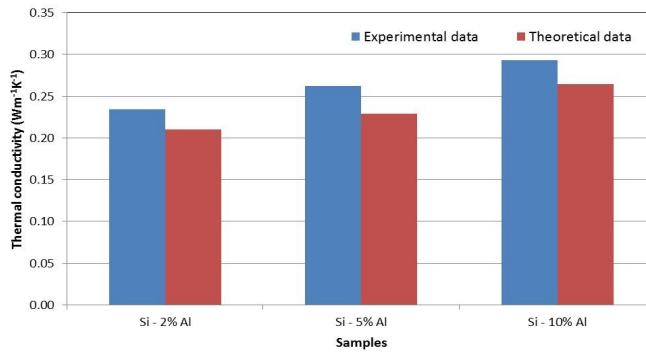


Figure 4.4: The experimental and theoretical thermal conductivity results for different volume proportions of aluminum.

### 4.3 BET analysis

The application of impregnation method causes changes inside the pore structure of silica gel. In order to evaluate the amount of changes, BET analysis has been performed for impregnated silica gel samples. Specific surface area of porous materials

are evaluated using BET theory in which nitrogen adsorption is measured as a function of relative pressure. The pore width and pore diameter of adsorbents are also obtained by this method. The BET tests were conducted for four samples of impregnated silica gel at METU central laboratory and results are given in Table 4.4 and Figures 4.5, 4.6 and 4.7. The samples have been dried at 100 °C for 16 hours before performing the experiments.

Table 4.4: BET test results for samples.

Samples	Sample weight (g)	Surface area ( $m^2 g^{-1}$ )	Pore Volume ( $cc g^{-1}$ )	Pore diameter (Å)	Pore width (Å)
Silica gel	0.0563	875	0.321	16.0	21.7
S20	0.0439	449	0.166	16.6	23.3
S40	0.048	257	0.0945	16.6	23.6
S60	0.0459	278	0.101	16.6	24.1

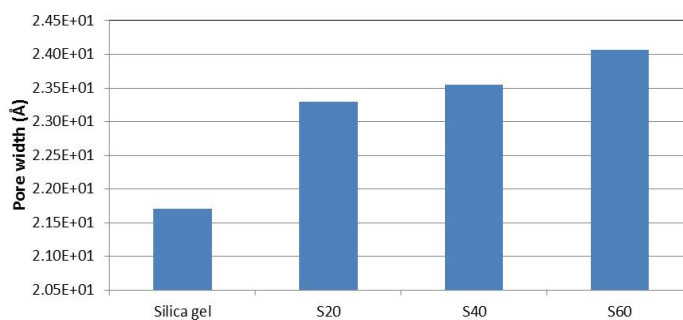


Figure 4.5: Pore width of the samples.

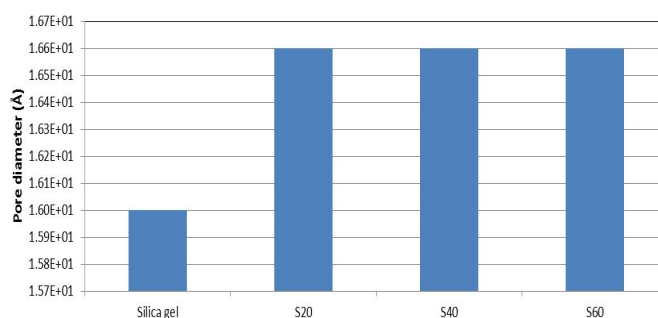


Figure 4.6: Pore diameter of the samples.

The results show that there is an increase in the amount of pore width of the samples by addition of  $CaCl_2$  amount in the solution. However, pore diameter has not changed for the different percentages of impregnated silica gel adsorbents. Overall, the surface area of the samples is decreased by impregnating  $CaCl_2$  into the pore structure of silica gel.

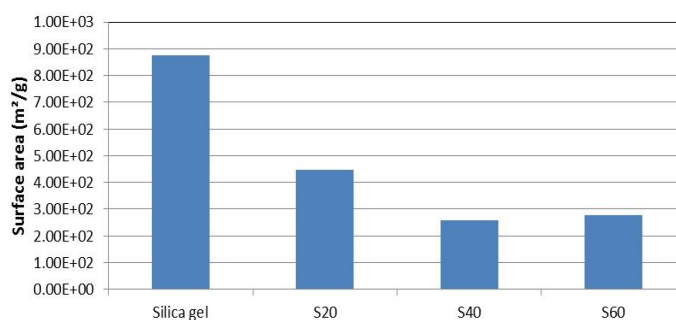


Figure 4.7: Surface area of the samples.

#### 4.4 Heat capacity analysis

The specific heat capacity of the impregnated silica gel adsorbents are determined at METU Central Laboratory. Specific heat capacity measurements were made by DSC (Differential Scanning Calorimetry) method in the temperature range 0-200 °C. DSC is a method in which the results for the amount of heat required to increase the temperature of a sample is compared with a reference as a function of temperature. Figures 4.8, 4.9, 4.10 and 4.11 show the heat capacity variations of samples with time. The results show that there is a slight decrease in the amount of specific heat capacity as the proportion of  $\text{CaCl}_2$  in the solution increases. Also, the reason behind the irregular behavior of the determined specific heat capacity at the right side of the Figures, is mainly due to the existence of some percentages of vaporized water which influence the exact calculations of the specific heat capacity. However, the values at lower temperatures can be assumed as the accurate specific heat capacity of the tested samples.

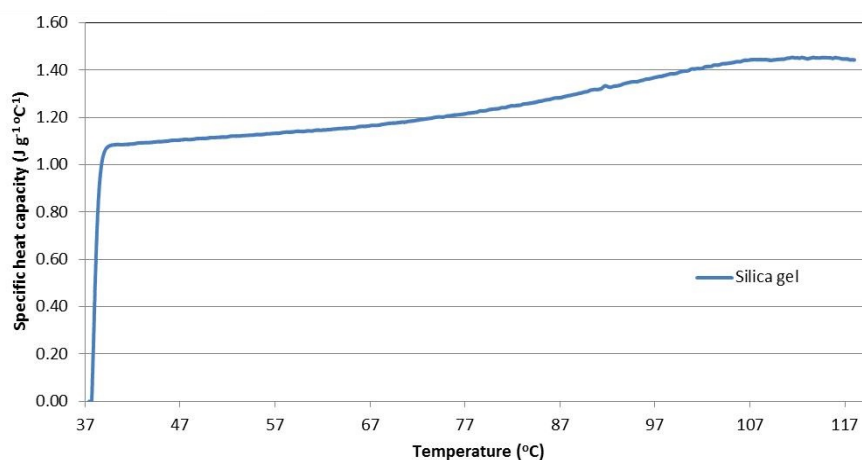


Figure 4.8: Heat capacity variations of pure silica gel with time.

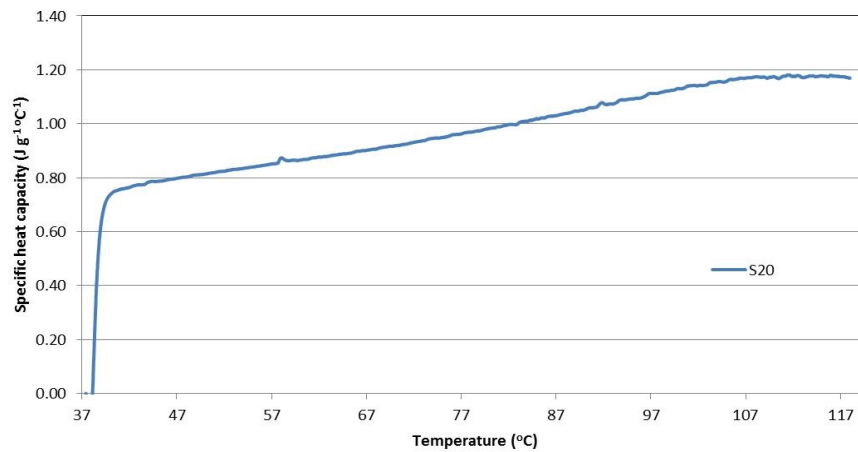


Figure 4.9: Heat capacity variations of S20 with time.

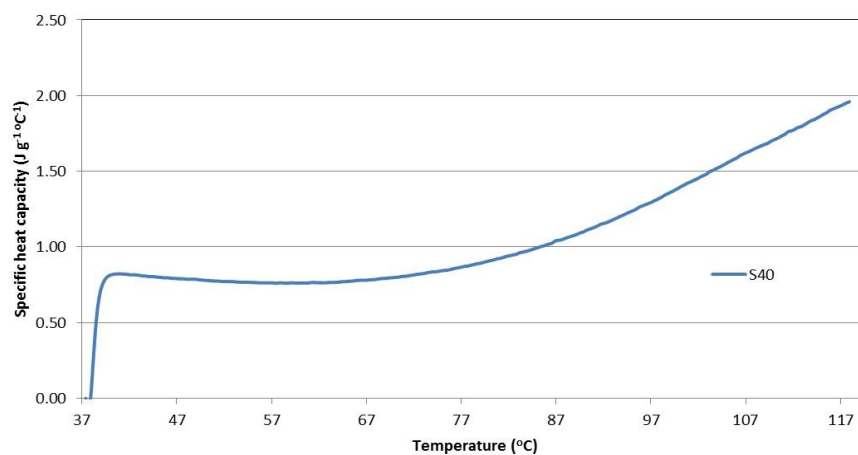


Figure 4.10: Heat capacity variations of S40 with time.

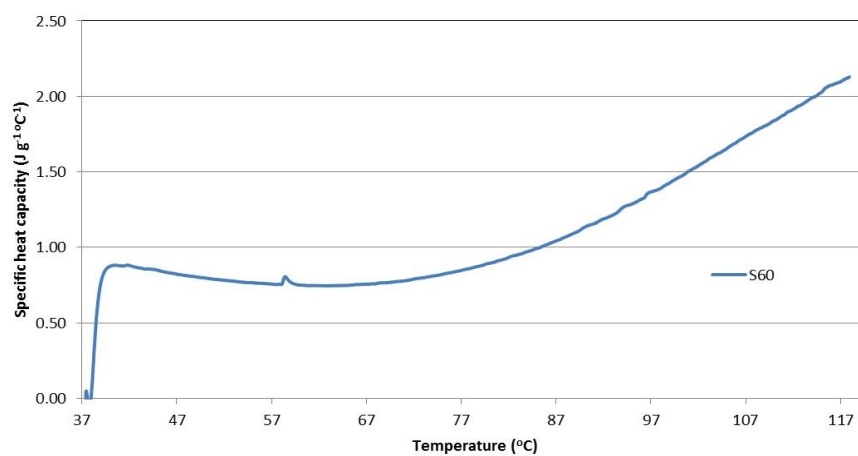


Figure 4.11: Heat capacity distribution of S60 with time.



## **CHAPTER 5**

# **INVESTIGATING THE INFLUENCE OF MODIFICATIONS ON THE PERFORMANCE OF AN ADSORPTION COOLING UNIT**

### **5.1 Introduction**

One of the objectives of this thesis is to experimentally investigate the influence of modified silica gel adsorbents in an adsorption cooling system. In this work, a previously established experimental set-up in Heat Transfer Laboratory at Mechanical Engineering Department, METU has been developed. For this purpose, several equipments have been supplied and the set-up is prepared for the adsorption tests. In this chapter, the set-up and components are described in detail. Also, the experiments procedure for adsorption cycle is expressed. Finally, temperature, pressure and water uptake amount distribution in the adsorption cycle are discussed and the results are compared for the prepared samples.

### **5.2 Description of the experimental set-up and components**

A schematic view of the experimental apparatus and its components is shown in Figure 5.1. The main components of the experimental set-up are: adsorbent bed, evaporator/condenser, water bath, oven, piping system and measurement devices. The information about these components are given in the following sections.

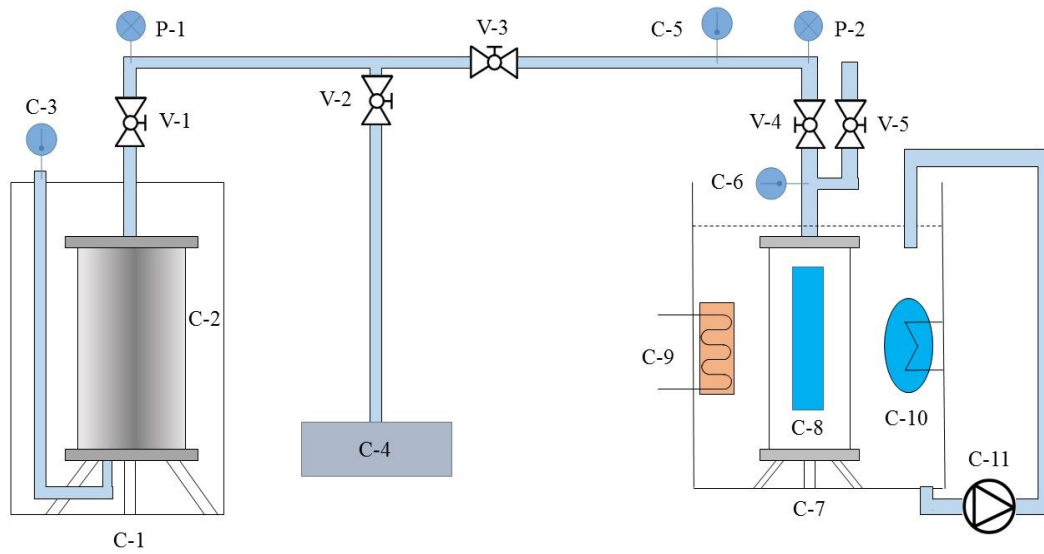


Figure 5.1: A schematic view of the experimental set-up (C-1 Oven; C-2 Adsorbent bed; C-3 Adsorbent bed thermocouple output; C-4 Vacuum pump; C-5 Pipe thermocouple output; C-6 Evaporator thermocouple output; C-7 Water bath; C-8 Evaporator/Condenser; C-9 V-C cooling system; C-10 Electrical heater; C-11 Circulation pump; V-1 ... 5 Vacuum valves; P-1,2 Pressure transducers).

### 5.2.1 Adsorbent bed

The outer and inner view of the adsorbent bed and its components are presented in Figure 5.2. The bed consists of a stainless steel cylinder, compression plate, spring, o-rings and top cover. The cylinder has 140 mm diameter and 250 mm length in which 3/5 of the volume is filled with adsorbents and the rest is a vapor gap. Also, for increasing the heat and mass transfer rate in the bed, 8 fins and 9 mass transfer tubes are placed in the positions shown in Figure 5.2.

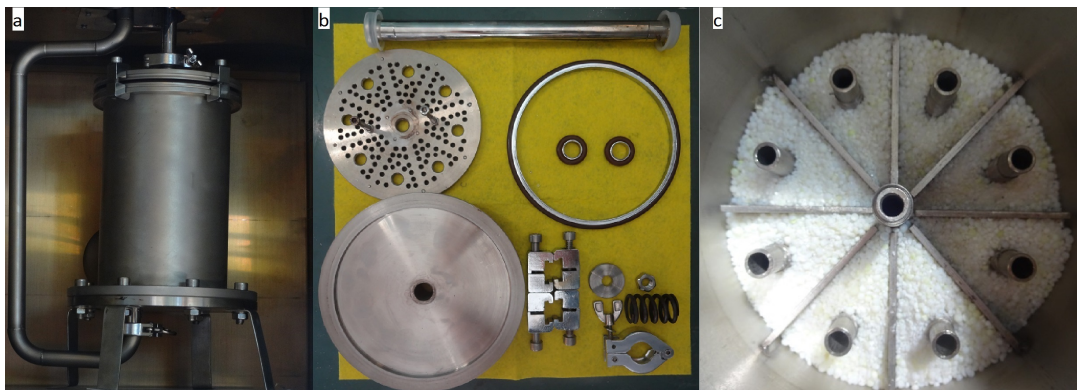


Figure 5.2: The outer and inner view of the adsorbent bed and its components.



The temperature distribution inside the bed is observed using a thermocouple installed at radii 46 mm from the center of the adsorbent bed and 97 mm from the bottom of the bed. After the adsorbents were filled inside and top cover was fastened securely, the bed is placed inside the oven to control the adsorbent's temperature accurately. Since the system works in vacuum condition, o-rings are used in every joint to prevent the air penetration to the system.

### 5.2.2 Evaporator/Condenser

An apparatus shown in Figure 5.3 was developed in the heat transfer laboratory as evaporator/condenser component. During adsorption process, this component works as evaporator and in desorption, the water is condensed inside this apparatus. The component consists of an 80 mm inner diameter and 100 mm outer diameter glass tube, with stainless steel top and bottom covers. The height of the tube is 30 mm. The change in the amount of water vaporized and condensed are measured during the adsorption and desorption processes, respectively. Also, two thermocouples are installed on top and bottom of the tube to observe the temperature distribution of water in liquid and gas phases. The evaporator/condenser is placed inside the water bath. The bath is filled with water and its temperature is controlled by a small vapor compression cooling unit and an electrical heater. A circulating pump is also utilized to keep the temperature of the bath in a uniform.



Figure 5.3: The photograph of the evaporator/condenser component used in the system.

### 5.2.3 Water bath and oven

Water bath contains three 1.5 kW electrical heaters and evaporator coil connected to a vapor compression cooling system. The temperature of the bed is also controlled uniformly inside the oven by using a blower. Two thermocouples measure the temperature of the oven and water bath which are connected to data acquisition system. A photograph of the water bath and oven is shown in Figure 5.4.



Figure 5.4: The photograph of the water bath and oven used in the system.

### 5.2.4 Piping system

The components of the adsorption system are connected to each other through a piping system. Also, to provide the vacuum conditions before the start of adsorption process, a two-stage Edwards rotary vane vacuum pump is used shown in Figure 5.5. Due to the condensation of water vapor during the adsorption cycle, the piping system is wrapped with a electrical heater tape. The temperature of the pipe is controlled using a thermocouple installed on the surface of the pipe.



Figure 5.5: The photograph of the rotary vacuum pump used in the system.

### 5.2.5 Measurement devices

Thermocouples, thermocouple feedthroughs and pressure transducers are the measurement devices used in cooling unit. The thermocouple feedthroughs are specifically used in vacuum systems to avoid the penetration of air to the system. Two pressure transducers are also installed on the system to control the pressure of adsorbent bed and evaporator/condenser components. The transducers were supplied from Omega Co. and are capable to measure the pressures in the range of 0-350 mbar accurately. A photograph of pressure transducer and thermocouple feedthroughs are shown in Figure 5.6.

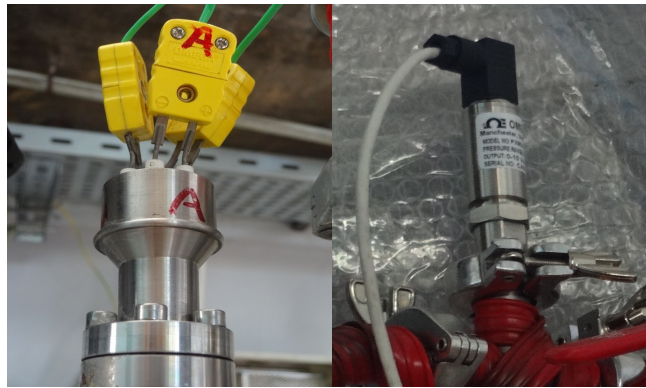


Figure 5.6: The photograph of thermocouple feedthroughs in the left and pressure transducer in the right.

Datataker DT800 is also used as data acquisition and control (DAQ) system. The thermocouples and pressure transducers are connected to DAQ which can be controlled using the user interface program installed on the computer. Delogger program is used to observe the data and send commands to DAQ system. The data are recorded every 5 seconds and saved in the computer's hard disk. A photograph of the DAQ system is shown in Figure 5.7.



Figure 5.7: The photograph of the DAQ system.

### 5.3 Experimental procedure

In the first step, the bed is filled with the adequate amount of adsorbent samples and prepared using the methods mentioned in previous chapters. Then the bed is put inside the oven and connected to the rest of the adsorption cycle through the piping system. The oven temperature is set at 90 °C. The evaporator is also prepared by pouring enough distilled water inside the glass tube. Also, the temperature of the water bath is set at 10 °C. The next and the most important step is to evacuate the adsorption system properly. The evacuation process consists of two sub steps. First, the vacuum pump is connected to the piping system under the valve V-4 and start to intake the air. After evacuating this part, the next step is to evacuate the rest of the system. Therefore, vacuum pump is connected to the piping system at valve V-2 and all valves except V-4 and V-5 are opened. This process continues until the pressure reaches to 3-5 mbar. The system is considered as in vacuum condition when the pressure distribution with time shows approximately same values in uniform manner after the vacuum pump is turned off. As the temperature of the bed is fixed at 90 °C, the valve V-2 is closed and V-4 is slowly cracked. Since the pressure of the system is below 10 mbar, the water inside the evaporator starts to vaporize. The vaporized water moves slowly toward the adsorption bed and adsorption process starts. Together with adsorption process, the water content inside the evaporator decreases and heat of adsorption exerted from this process slightly increase the temperature of the bed. The adsorption process is continued until the equilibrium condition is achieved inside the system. After reaching equilibrium condition, the oven temperature is set at 60 °C. The adsorption process starts again as the bed pressure decreases to evaporator pressure. This process is repeated for the temperatures between 60 °C and 40 °C. The amount of water decreased inside the evaporator is recorded every 20-40 minutes and used for calculating the total water uptake of the adsorbents.

After the adsorption process finishes and no more adsorption occurs, the temperature of the adsorbent bed is increased to 90 °C inside the oven and desorption process starts as the pressure of the bed reaches to condenser pressure. As the temperature of the adsorbent bed increases, more water is desorbed from the surface of the adsorbents. The desorption process continues until no more water goes back to the condenser.

## 5.4 Result and discussions

The results have been obtained for temperature, pressure and water uptake of the tested materials. The temperature and pressure distribution in the adsorbent bed and evaporator demonstrates the process of adsorption in every step of cycle time. As shown in Figure 5.8, there is a slight increase in the temperature of the bed as the adsorption occurs at 90 °C as the valve V-4 is cracked. The same behavior can be also inferred from the results for evaporator temperature and system pressure. The system reaches to equilibrium approximately one hour after the start of adsorption process. The adsorption process between 90 °C to 60 °C and 60 °C to 40 °C is also shown for three samples. The bed temperature is set constant for different samples and therefore cycle time may change for samples. Temperature and pressure distribution for impregnated silica gel and aluminum mixture are illustrated in Figures 5.9 and 5.10.

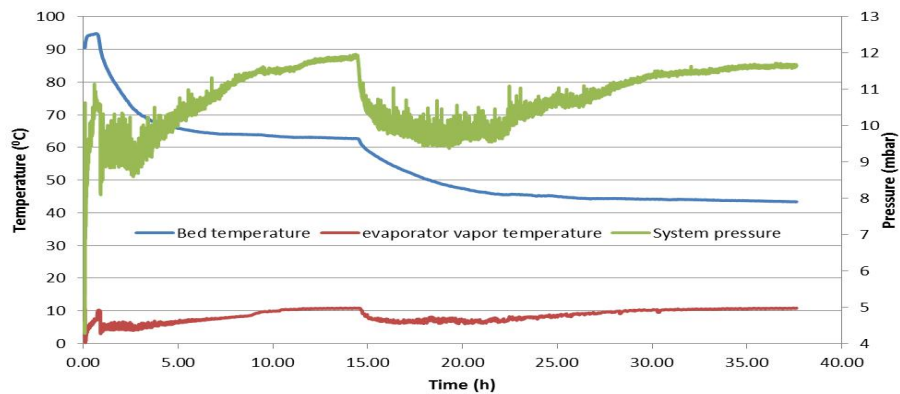


Figure 5.8: Temperature and pressure distribution in adsorption process for silica gel.

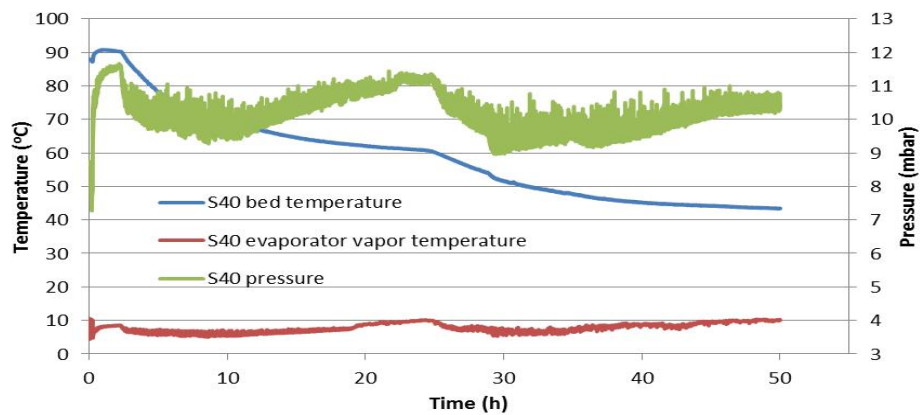


Figure 5.9: Temperature and pressure distribution in adsorption process for S40.

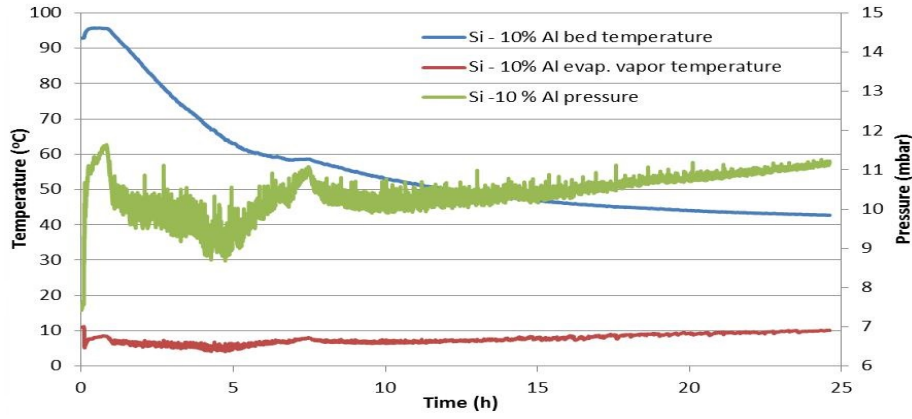


Figure 5.10: Temperature and pressure distribution in adsorption for Si-10% Al.

The main objective of this work is to determine the water uptake capacity of impregnated silica gel and influence of metal additives on water uptake of silica gel. For this purpose, the three samples have been prepared and tested using the mentioned procedure. The water uptake amount for three samples are shown in Figures 5.11, 5.12 and 5.13.

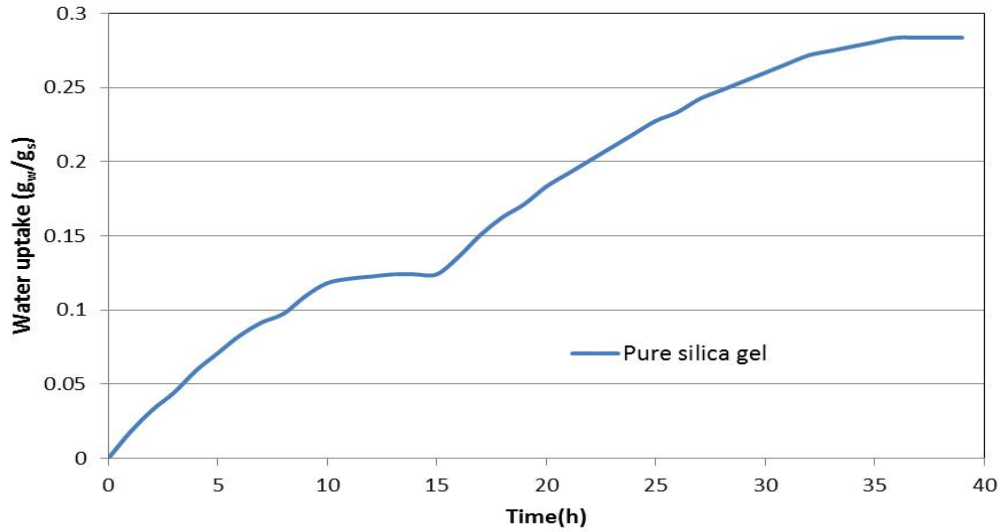


Figure 5.11: Water uptake distribution in adsorption process for silica gel.

The results indicated in figures show that pure silica gel has the water uptake capacity of  $0.283 \text{ kg}_w \text{ kg}_s^{-1}$ . For impregnated silica gel with 40% calcium chloride, this amount reaches to  $0.566 \text{ kg}_w \text{ kg}_s^{-1}$ . On the other hand, results in Figure 5.13 show that adding 10% aluminum to the bed reduces the water uptake capacity to  $0.23 \text{ kg}_w \text{ kg}_s^{-1}$  which is mainly due to the reduction in the amount of adsorbents. Increas-

ing the mass transfer resistances can also limit the water vapor access to all adsorbents and reduce the water adsorption in the bed.

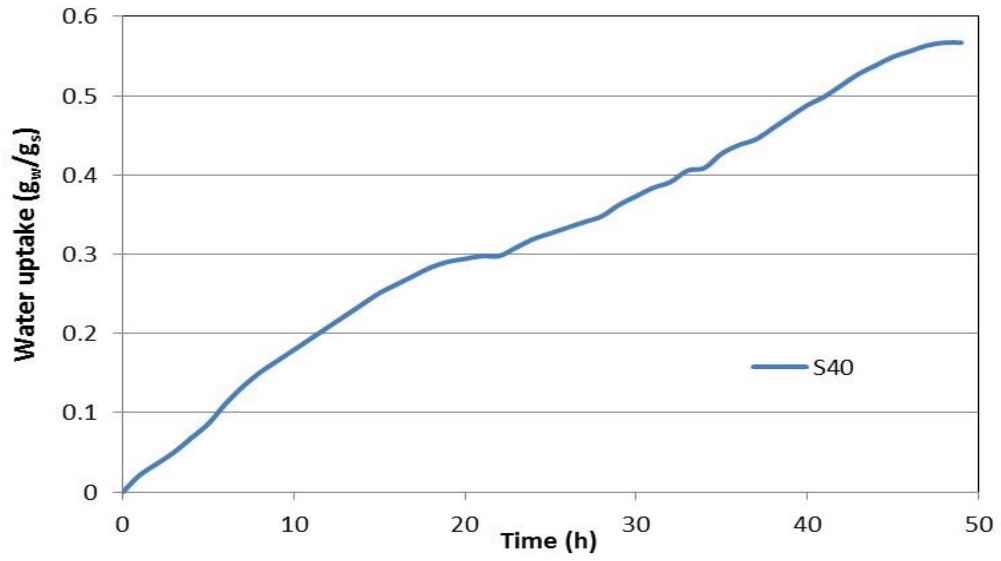


Figure 5.12: Water uptake distribution in adsorption process for S40.

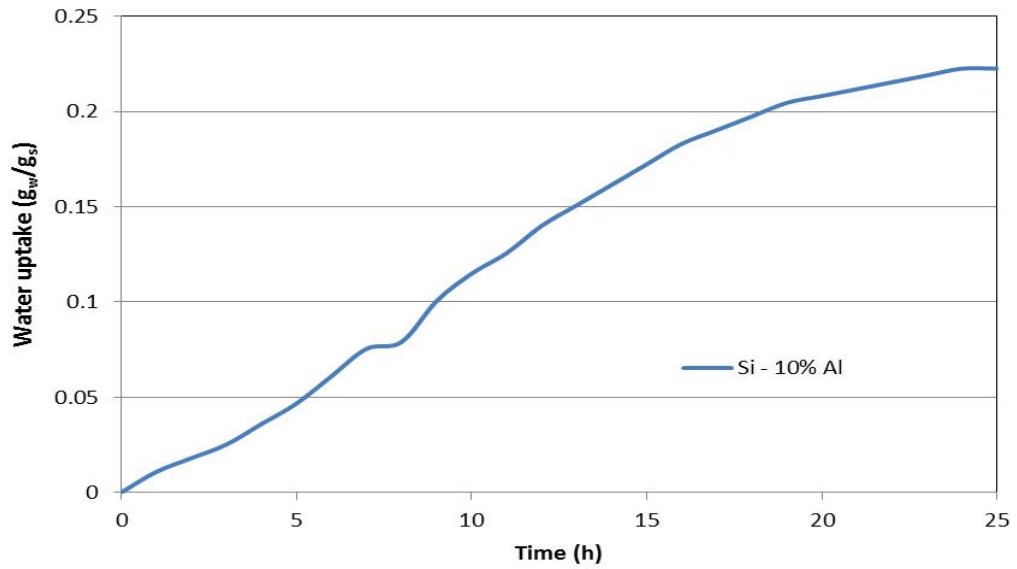


Figure 5.13: Water uptake distribution in adsorption process for Si-10% Al.





## CHAPTER 6

### CONCLUSIONS AND RECOMMENDATIONS

This thesis is an integration of three related studies. Firstly, a one-dimensional numerical model has been developed and solved in COMSOL Multiphysics to investigate the influence of thermal conductivity on the adsorption and desorption processes inside the bed. Secondly, silica gel adsorbent is modified by adding metal pieces and impregnation method to increase the heat and mass transfer and water uptake capacity of the adsorbent bed, respectively. Thirdly, the thermo physical properties and water uptake capacity of the modified materials are tested in a set of experimental studies.

The results from one-dimensional model show that the bed with higher thermal conductivity demonstrates better thermal behavior and also reaches to equilibrium in shorter time. In chapter three, the samples prepared using impregnation and metal additive methods. The new impregnated adsorbent has different shape and color in comparison to conventional silica gel. The thermo physical properties of samples are determined in chapter four. In the first step, thermal conductivity calculated for all samples. The results show up to 37.8% improvement in thermal conductivity of the mixture with 10% volume fraction of aluminum. Also, a slight increment can be observed in thermal conductivity of silica gel adsorbent modified by confining  $\text{CaCl}_2$  into its pores. Next, heat capacity of the impregnated samples was determined using the DSC test conducted in central laboratory at METU. As a result, heat capacity of samples decrease as the proportion of  $\text{CaCl}_2$  in the solution increases. The pore size and surface area of the prepared samples have also been determined using the BET analysis in central laboratory at METU. The impregnated materials show higher pore width and diameter in comparison to unmodified silica gel. The BET results show

that the mass transfer rate of the impregnated silica gel adsorbents is increased in comparison to conventional silica gel. However, the surface area of the impregnated silica gel has been decreased. In the last study, new samples have been experimentally tested in an adsorption cooling unit. The aim of this experiment is to investigate the influence of modifications on the water uptake capacity of the adsorbent. The results show that the water uptake capacity of impregnated silica gel in 40%  $\text{CaCl}_2$  solution is approximately twice that of the conventional silica gel. On the other hand, adding 10% volume fraction of aluminum additive reduces the water uptake capacity of the bed by 18.7% when compared to silica gel.

As can be inferred from the results, adding metal pieces to the bed increases the thermal behavior of the bed significantly. However, at the same time, metal additives affect the water uptake capacity of the bed. The solution to this problem is given by impregnation method. The results obtained from the adsorption cooling unit show that the presence of  $\text{CaCl}_2$  in the structure of silica gel increases the water uptake capacity significantly.

As future work, the impact of metal additives on the performance of impregnated silica gel adsorbents can be investigated. In this case, both thermal behavior and adsorption capacity of the bed increase simultaneously. Also, two-dimensional or three-dimensional models should be developed to investigate the impact of different parameters and working conditions on the performance of the cooling unit. To obtain better results, various types of impregnated materials can be fabricated using different chemical adsorbents. The properties and performance of the new adsorbents can be determined using the experimental set-up and test facilities prepared.

## REFERENCES

- [1] Hasan Demir, Moghtada Mobedi, and Semra Ülkü. A review on adsorption heat pump: Problems and solutions. *Renewable and Sustainable Energy Reviews*, 12(9):2381–2403, December 2008.
- [2] Ahmed A. Askalany, M. Salem, I.M. Ismael, A.H.H. Ali, M.G. Morsy, and Bidyut B. Saha. An overview on adsorption pairs for cooling. *Renewable and Sustainable Energy Reviews*, 19:565–572, March 2013.
- [3] Ismail Solmus. *AN EXPERIMENTAL STUDY ON THE PERFORMANCE OF AN ADSORPTION.pdf*. PhD thesis, MIDDLE EAST TECHNICAL UNIVERSITY, 2011.
- [4] Worldwide energy consumption projections in 2040. <http://www.eia.gov/totalenergy/data/monthly>, July 2013.
- [5] Biplab Choudhury, Bidyut Baran Saha, Pradip K. Chatterjee, and Jyoti Prakash Sarkar. An overview of developments in adsorption refrigeration systems towards a sustainable way of cooling. *Applied Energy*, 104:554–567, April 2013.
- [6] Douglas M. Ruthven. *Principles of Adsorption and Adsorption Processes*. John Wiley & Sons, June 1984.
- [7] L.W. Wang, R.Z. Wang, and R.G. Oliveira. A review on adsorption working pairs for refrigeration. *Renewable and Sustainable Energy Reviews*, 13(3):518–534, April 2009.
- [8] José Maurício Gurgel and Rogerio P. Klüppel. Thermal conductivity of hydrated silica-gel. *The Chemical Engineering Journal and the Biochemical Engineering Journal*, 61(2):133–138, February 1996.
- [9] T.S. Ge, Y. Li, R.Z. Wang, and Y.J. Dai. A review of the mathematical models for predicting rotary desiccant wheel. *Renewable and Sustainable Energy Reviews*, 12(6):1485–1528, August 2008.
- [10] Hasan Demir, Moghtada Mobedi, and Semra Ülkü. The use of metal piece additives to enhance heat transfer rate through an unconsolidated adsorbent bed. *International Journal of Refrigeration*, 33(4):714–720, June 2010.
- [11] Ahmet Caglar. *DESIGN AND CONSTRUCTION OF THE ADSORBENT BED OF A THERMAL WAVE ADSORPTION COOLING CYCLE*. PhD thesis, MIDDLE EAST TECHNICAL UNIVERSITY, 2012.

- [12] S. G. Wang, R. Z. Wang, and X. R. Li. Research and development of consolidated adsorbent for adsorption systems. *Renewable Energy*, 30(9):1425–1441, July 2005.
- [13] K.R. Ullah, R. Saidur, H.W. Ping, R.K. Akikur, and N.H. Shuvo. A review of solar thermal refrigeration and cooling methods. *Renewable and Sustainable Energy Reviews*, 24:499–513, August 2013.
- [14] Napoleon Enteria and Kunio Mizutani. The role of the thermally activated desiccant cooling technologies in the issue of energy and environment. *Renewable and Sustainable Energy Reviews*, 15(4):2095–2122, May 2011.
- [15] T. F. Qu, R. Z. Wang, and W. Wang. Study on heat and mass recovery in adsorption refrigeration cycles. *Applied Thermal Engineering*, 21(4):439–452, March 2001.
- [16] Xiaolin Wang and H. T. Chua. A comparative evaluation of two different heat-recovery schemes as applied to a two-bed adsorption chiller. *International Journal of Heat and Mass Transfer*, 50(3–4):433–443, February 2007.
- [17] R. Z. Wang and R. G. Oliveira. Adsorption refrigeration—an efficient way to make good use of waste heat and solar energy. *Progress in Energy and Combustion Science*, 32(4):424–458, 2006.
- [18] S. L. Li, Z. Z. Xia, J. Y. Wu, J. Li, R. Z. Wang, and L. W. Wang. Experimental study of a novel CaCl<sub>2</sub>/expanded graphite-NH<sub>3</sub> adsorption refrigerator. *International Journal of Refrigeration*, 33(1):61–69, January 2010.
- [19] Michael J. Tierney. Feasibility of driving convective thermal wave chillers with low-grade heat. *Renewable Energy*, 33(9):2097–2108, September 2008.
- [20] W. Zheng, W. M. Worek, and G. Nowakowski. Effect of operating conditions on the performance of two-bed closed-cycle solid-sorption heat pump systems. *Journal of Solar Energy Engineering*, 117(3):181–186, August 1995.
- [21] Clito F.A. Afonso. Recent advances in building air conditioning systems. *Applied Thermal Engineering*, 26(16):1961–1971, November 2006.
- [22] M. Z. I. Khan, K. C. A. Alam, B. B. Saha, A. Akisawa, and T. Kashiwagi. Performance evaluation of multi-stage, multi-bed adsorption chiller employing re-heat scheme. *Renewable Energy*, 33(1):88–98, January 2008.
- [23] K. Sumathy, K.H. Yeung, and Li Yong. Technology development in the solar adsorption refrigeration systems. *Progress in Energy and Combustion Science*, 29(4):301–327, 2003.
- [24] A. Ramzy K., R. Kadoli, and T. P. Ashok Babu. Improved utilization of desiccant material in packed bed dehumidifier using composite particles. *Renewable Energy*, 36(2):732–742, February 2011.

- [25] S. Misha, S. Mat, M.H. Ruslan, and K. Sopian. Review of solid/liquid desiccant in the drying applications and its regeneration methods. *Renewable and Sustainable Energy Reviews*, 16(7):4686–4707, September 2012.
- [26] Donald A. Nield and Adrian Bejan. *Convection in Porous Media*. Springer New York, January 2013.
- [27] F. Duval, F. Fichot, and M. Quintard. A local thermal non-equilibrium model for two-phase flows with phase-change in porous media. *International Journal of Heat and Mass Transfer*, 47(3):613–639, January 2004.
- [28] M. A. Alghoul, M. Y. Sulaiman, B. Z. Azmi, and M. Abd. Wahab. Advances on multi-purpose solar adsorption systems for domestic refrigeration and water heating. *Applied Thermal Engineering*, 27(5–6):813–822, April 2007.
- [29] Dechang Wang, Jipeng Zhang, Xiaoliang Tian, Dawei Liu, and K. Sumathy. Progress in silica gel–water adsorption refrigeration technology. *Renewable and Sustainable Energy Reviews*, 30:85–104, February 2014.
- [30] Marc Linder, Rainer Mertz, and Eckart Laurien. Experimental results of a compact thermally driven cooling system based on metal hydrides. *International Journal of Hydrogen Energy*, 35(14):7623–7632, July 2010.
- [31] Adrian Bejan. *Design with Constructal Theory*. Wiley, Hoboken, N.J, 1 edition edition, September 2008.
- [32] G. Restuccia, A. Freni, F. Russo, and S. Vasta. Experimental investigation of a solid adsorption chiller based on a heat exchanger coated with hydrophobic zeolite. *Applied Thermal Engineering*, 25(10):1419–1428, July 2005.
- [33] Kuei-Sen Chang, Mai-Tzu Chen, and Tsair-Wang Chung. Effects of the thickness and particle size of silica gel on the heat and mass transfer performance of a silica gel-coated bed for air-conditioning adsorption systems. *Applied Thermal Engineering*, 25(14–15):2330–2340, October 2005.
- [34] G. Restuccia, A. Freni, and G. Maggio. A zeolite-coated bed for air conditioning adsorption systems: parametric study of heat and mass transfer by dynamic simulation. *Applied Thermal Engineering*, 22(6):619–630, April 2002.
- [35] A. Rezk, R. K. Al-Dadah, S. Mahmoud, and A. Elsayed. Effects of contact resistance and metal additives in finned-tube adsorbent beds on the performance of silica gel/water adsorption chiller. *Applied Thermal Engineering*, 53(2):278–284, May 2013.
- [36] D. C. Wang, Z. Z. Xia, J. Y. Wu, R. Z. Wang, H. Zhai, and W. D. Dou. Study of a novel silica gel–water adsorption chiller. part i. design and performance prediction. *International Journal of Refrigeration*, 28(7):1073–1083, November 2005.

- [37] D. C. Wang, J. Y. Wu, Z. Z. Xia, H. Zhai, R. Z. Wang, and W. D. Dou. Study of a novel silica gel–water adsorption chiller. part II. experimental study. *International Journal of Refrigeration*, 28(7):1084–1091, November 2005.
- [38] Zisheng Lu, Ruzhu Wang, and Zaizhong Xia. Experimental analysis of an adsorption air conditioning with micro-porous silica gel–water. *Applied Thermal Engineering*, 50(1):1015–1020, January 2013.
- [39] Z. S. Lu, R. Z. Wang, Z. Z. Xia, Q. B. Wu, Y. M. Sun, and Z. Y. Chen. An analysis of the performance of a novel solar silica gel–water adsorption air conditioning. *Applied Thermal Engineering*, 31(17–18):3636–3642, December 2011.
- [40] C. J. Chen, R. Z. Wang, Z. Z. Xia, J. K. Kiplagat, and Z. S. Lu. Study on a compact silica gel–water adsorption chiller without vacuum valves: Design and experimental study. *Applied Energy*, 87(8):2673–2681, August 2010.
- [41] Y. L. Liu, R. Z. Wang, and Z. Z. Xia. Experimental performance of a silica gel–water adsorption chiller. *Applied Thermal Engineering*, 25(2–3):359–375, February 2005.
- [42] Dechang Wang, Jipeng Zhang, Qirong Yang, Na Li, and K. Sumathy. Study of adsorption characteristics in silica gel–water adsorption refrigeration. *Applied Energy*, 113:734–741, January 2014.
- [43] Dechang Wang, Jipeng Zhang, Yanzhi Xia, Yanpei Han, and Shuwei Wang. Investigation of adsorption performance deterioration in silica gel–water adsorption refrigeration. *Energy Conversion and Management*, 58:157–162, June 2012.
- [44] Hui T. Chua, Kim C. Ng, Anutosh Chakraborty, Nay M. Oo, and Mohamed A. Othman. Adsorption characteristics of silica gel + water systems. *Journal of Chemical & Engineering Data*, 47(5):1177–1181, September 2002.
- [45] I. S. Glaznev and Yu. I. Aristov. The effect of cycle boundary conditions and adsorbent grain size on the water sorption dynamics in adsorption chillers. *International Journal of Heat and Mass Transfer*, 53(9–10):1893–1898, April 2010.
- [46] R. Narayanan, W.Y. Saman, S.D. White, and M. Goldsworthy. Comparative study of different desiccant wheel designs. *Applied Thermal Engineering*, 31(10):1613–1620, July 2011.
- [47] Dhanes Charoensupaya and William M. Worek. Parametric study of an open-cycle adiabatic, solid, desiccant cooling system. *Energy*, 13(9):739–747, September 1988.
- [48] İsmail Solmuş, D. Andrew S. Rees, Cemil Yamalı, Derek Baker, and Bilgin Kafatanoğlu. Numerical investigation of coupled heat and mass transfer inside the

- adsorbent bed of an adsorption cooling unit. *International Journal of Refrigeration*, 35(3):652–662, May 2012.
- [49] Yu. I Aristov, G Restuccia, G Cacciola, and V. N Parmon. A family of new working materials for solid sorption air conditioning systems. *Applied Thermal Engineering*, 22(2):191–204, February 2002.
  - [50] G. Restuccia, A. Freni, S. Vasta, and Yu Aristov. Selective water sorbent for solid sorption chiller: experimental results and modelling. *International Journal of Refrigeration*, 27(3):284–293, May 2004.
  - [51] K. Daou, R. Z. Wang, G. Z. Yang, and Z. Z. Xia. Theoretical comparison of the refrigerating performances of a  $\text{CaCl}_2$  impregnated composite adsorbent to those of the host silica gel. *International Journal of Thermal Sciences*, 47(1):68–75, January 2008.
  - [52] K. Daou, R. Z. Wang, Z. Z. Xia, and G. Z. Yang. Experimental comparison of the sorption and refrigerating performances of a  $\text{CaCl}_2$  impregnated composite adsorbent and those of the host silica gel. *International Journal of Refrigeration*, 30(1):68–75, January 2007.
  - [53] L.W. Wang, R.Z. Wang, Z.S. Lu, C.J. Chen, K. Wang, and J.Y. Wu. The performance of two adsorption ice making test units using activated carbon and a carbon composite as adsorbents. *Carbon*, 44(13):2671–2680, November 2006.
  - [54] C. Y. Tso and Christopher Y. H. Chao. Activated carbon, silica-gel and calcium chloride composite adsorbents for energy efficient solar adsorption cooling and dehumidification systems. *International Journal of Refrigeration*, 35(6):1626–1638, September 2012.
  - [55] E.S. Dettmer, B.M. Romenesko, Jr. Charles, H.K., B.G. Carkhuff, and D.J. Merrill. Steady state thermal conductivity measurements of AlN and SiC substrate materials. In *Electronic Components Conference, 1989. Proceedings., 39th*, pages 551–556, May 1989.
  - [56] Jianfeng Wang, James K. Carson, Mike F. North, and Donald J. Cleland. A new structural model of effective thermal conductivity for heterogeneous materials with co-continuous phases. *International Journal of Heat and Mass Transfer*, 51(9–10):2389–2397, May 2008.